"DEVELOPMENT OF INTELLIGENT ALGORITHMS FOR DIAGNOSIS OF BRAIN ABNORMALITY AND DISEASES FROM MRI IMAGES"

SYNOPSIS OF THE THESIS
TO BE SUBMITTED TO MANGALORE UNIVERSITY
FOR THE AWARD OF DEGREE OF

DOCTOR OF PHILOSOPHY

IN

ELECTRONICS

BY
JOSE ALEX MATHEW

UNDER THE GUIDANCE OF
Dr. A. M. KHAN

MANGALORE UNIVERSITY

FACULTY OF SCIENCE AND TECHNOLOGY

DEPARTMENT OF P G STUDIES AND RESEARCH IN ELECTRONICS

MANGALAGANGOTRI – 574 199, INDIA

1. INTRODUCTION

1.1 Overview

Intelligent diagnostic Imaging System (IDIS) is a developing imaging modality that is beginning to show promise of detecting and characterizing abnormalities of the brain. The abnormalities of the brain are due to Intracranial Neoplasm, Cerebral Infections and Inflammations, Stroke, Cerebral Aneurysms, Vascular Malformations, Central Nervous System Trauma and Neurodegenerative Disorders. This work is concerned with the development of image processing tools and intelligent algorithms that will automatically detect the abnormalities of the brain and diagnosis of the abnormalities based on the structural information gathered from the images. This system helps to get information about disease and abnormality at the time of MRI scan if the system is assembled properly.

Graphical User Interface (GUI) has been developed and utilized to see the result of a diagnostic Imaging system in an easy way. In GUI, the abnormalities are extracted and identified by comparing the patient's slice images with normal slice image. Recognition of abnormality in an MRI image is a tedious task. First, abnormalities are extracted from different slices of a patient and compared with normal slices. Then each of the images with abnormality is compared with images in the abnormality image data set to identify and recognize the abnormalities. Finally a GUI is used for reading the image slice by slice, extraction of the abnormality and displaying the result.

The purpose of abnormality extraction is to understand and identify the abnormality which is very helpful for the physician to gain knowledge of the severity of the disease. Region based segmentation is used for this purpose. In abnormality extraction, the threshold detection is very important and it can be considered as the key feature of the Intelligent Diagnostic Imaging System. Image segmentation means partitioning an image into meaningful regions with respect to a particular application. The segmentation is based on measurements taken from the image and might be grey level, colour, texture, depth or motion. Usually image segmentation is an initial and vital step in a series of processes aimed at overall image understanding. Different algorithms are used for T1 and T2 MRI Images. MATLAB tools are used to do the segmentation. The intensity level of a particular abnormality is same in an MRI image slice. It can be iso-intense, hypo-intense or hyper-intense.

Medical image segmentation is generally difficult because often Noise-to-signal ratio is 10%. This is ten times the Noise-to-signal ratio of camera images. Medical images are often textured in complex ways and relatively poorly sampled. Many pixels contain more than one tissue type. This is called Partial Volume Effect. Objects of interest have complex shapes and the signs of clinical interest are very subtle.

In this work, the abnormality has been extracted using different segmentation methods like Region Growing, Region splitting and Merging and Marker-Controlled Watershed Segmentation. Then most pertinent segmentation method is selected and GUI is developed to see the abnormality and diagnose the abnormalities. After getting the information of abnormalities from the developed algorithm, the results are compared with the doctor's diagnosis report.

1.2 Magnetic Resonant Imaging (MRI)

The human body is primarily fat and water. Fat and water have many hydrogen atoms which make the human body approximately 63% hydrogen atoms. Proton of the hydrogen atom of human body acts as a magnetic dipole [1]. In the absence of an external magnetic field, magnetic dipoles are randomly oriented, resulting zero net magnetic fields. The introduction of an external magnetic field (B_0), forces the magnetic dipole to align in one of the two states: parallel (low energy) or anti-parallel (high energy). A small excess in the parallel direction results in a nonzero net magnetic field (M). For convenience, B_0 is along the z axis, so M is also along z axis. The transverse plane is perpendicular to the main field and contains x and y axis. For spin-echo imaging, 90-degree RF pulse is applied. M is flipped from the z axis to transverse plane. This transverse component of the M is entirely responsible for the MRI signal. M is returned to the equilibrium state by releasing energy called T1 relaxation (longitudinal). Immediately after the 90-degree RF pulse, the magnetic moments are located in the transverse plain. Transverse (xy) magnetization suddenly decays constitute T2 relaxation (transverse). Fluid Attenuating Inversion Recovery (FLAIR) imaging technique is used to enhance the contrast.

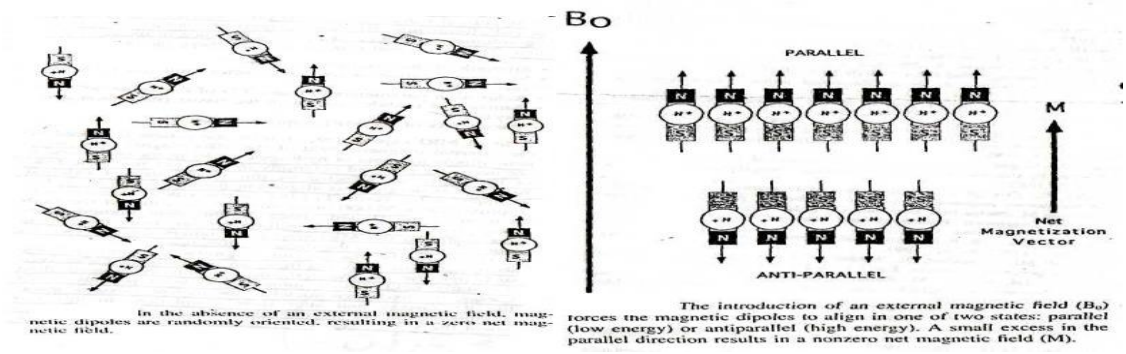

In the absence of an external magnetic field, magnetic dipoles are randomly oriented, resulting in a zero net magnetic field.

The introduction of an external magnetic field (B_0) forces the magnetic dipoles to align in one of two states: parallel (low energy) or antiparallel (high energy). A small excess in the parallel direction results in a nonzero net magnetic field (M).

Figure 1 a, b: Basics of MRI

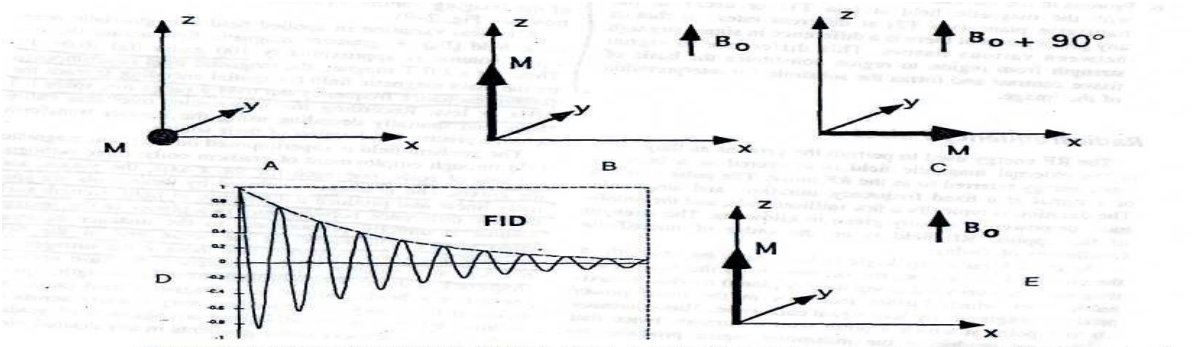

Diagrammatic representation of a basic MRI experiment. *A*, In the absence of an external magnetic field, net magnetization (M) is zero. *B*, Net magnetization is created by the application of an external static magnetic field (B_0). *C*, The application of energy, in the form of a 90-degree radiofrequency (RF) pulse, "tips" the magnetization vector onto the x-y plane. *D*, The precessing magnetization decays exponentially back to equilibrium (+ z). The amplitude of the x-y component of the magnetization versus time

Figure 2: Working of MRI with the application of static field and 90^0 radio pulse. For spin-echo imaging, 90-degree RF pulse is applied. M is flipped from the z axis to transverse plane. This transverse component of the M is entirely responsible for the MRI signal

The intensity of a pixel is proportional to the NMR signal intensity of the contents of the corresponding volume element or voxel of the object being imaged .MRI images are categorized in to mainly T1 and T2 images [2]. Pulse Sequences for MRI Imaging comprising of Spin-echo, Inversion recovery and Gradient-echo sequences. Spin-echo pulse sequences and Fluid Attenuating Inversion Recovery (FLAIR) sequences comes under T1 mode of scanning. Turbo Spin-echo sequences come under T2. Each type of imaging can be

done either on axial, sagittal or coronal axes. Normal slice thickness is 5 mm for MRI scans. So for a person, there are about twenty images under each axial, coronal and sagittal axes and grand total of approximately two hundred images.

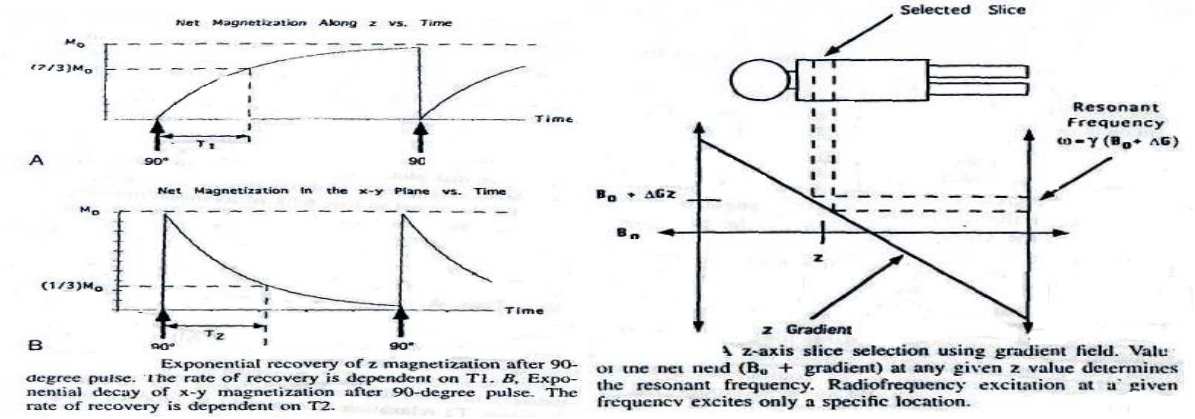

Exponential recovery of z magnetization after 90-degree pulse. The rate of recovery is dependent on T1. *B*, Exponential decay of x-y magnetization after 90-degree pulse. The rate of recovery is dependent on T2.

A z-axis slice selection using gradient field. Value of the net field (B_0 + gradient) at any given z value determines the resonant frequency. Radiofrequency excitation at a given frequency excites only a specific location.

Figure 3 a: T1 relaxation (longitudinal) and T2 relaxation (transverse), b: Spatial localization

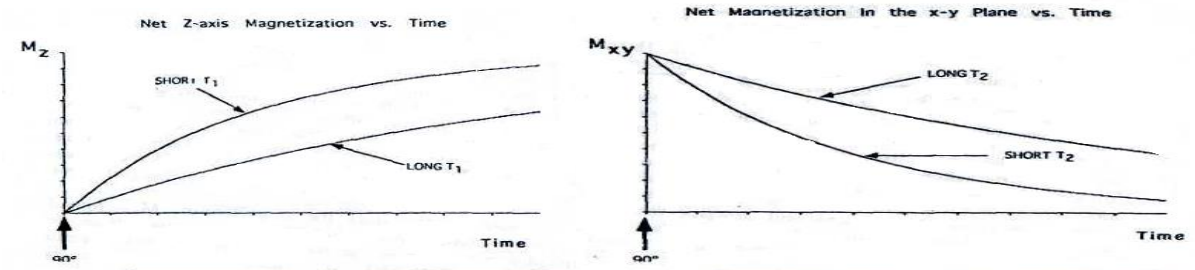

Exponential recovery of z magnetization after 90-degree pulse for two substances. The difference between the two curves determines contrast.

Exponential decay of x-y magnetization after 90-degree pulse for two substances. The difference between the two curves determines contrast.

Figure 4 a: Z-axis magnetization, b: X-Y plane magnetization

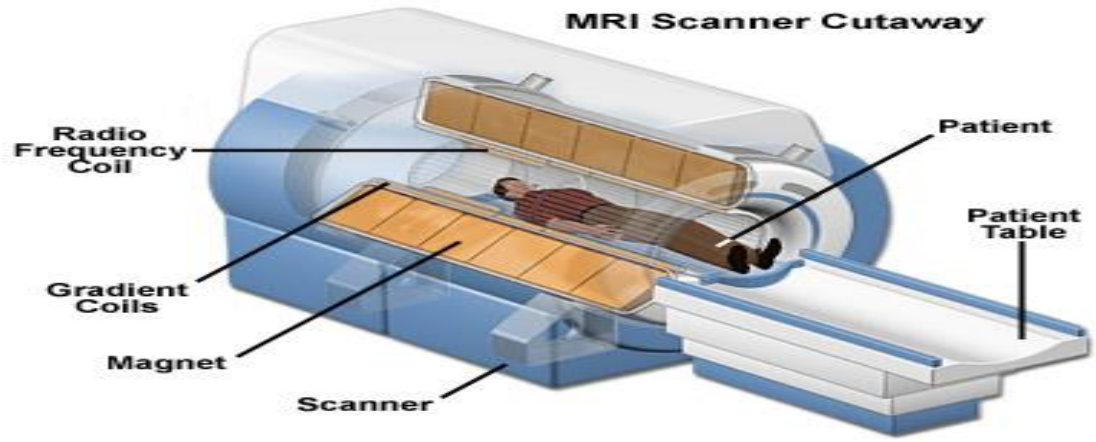

Figur 4c: MRI Scanner

Major components of an MRI scanner

i) A static magnetic field.

- The magnet is the largest and most expensive component of the scanner, and the remainder of the scanner is built around it.

ii) An RF transmitter and receiver

- RF transmission system consists of a RF synthesizer, power amplifier and the transmitting coil. This is usually built into the body of the scanner.
- The receiver consists of the coil, pre-amplifier and signal processing system.

iii) Three orthogonal, controllable magnetic gradients.

- Magnetic gradients are generated by three orthogonal coils, oriented in the x, y and z directions of the scanner. These are usually resistive electromagnets powered by sophisticated amplifiers which permit rapid and precise adjustments to their field strength and direction.

2. REVIEW OF PAST WORK IN AREA

A detailed study of medical imaging, MRI techniques and analysis of MRI data was carried out from the year 1996 to 2010 to understand the techniques for abnormality extraction and diagnosis. It is discussed as follows.

2.1 Segmentation

In 1996, Gregory A. Hance and group developed a computer vision system for skin cancer diagnosis [3]. In 1996, N. Manousakas and group used Split-and-merge techniques using homogeneity measures for segmentation [4]. In 2003, Koen Van Leemput and group present a statistical framework for PV segmentation that encompasses and extends existing techniques [5]. In 2003, Nilanjan Ray and group developed an active contour model that provides a smooth boundary and accurately captures the high curvature features of the lung cavities from the 1 H MR images for lung segmentation [6]. In 2003, Yoshinobu Sato and group investigated the fundamental limits on the accuracy of thickness determination in MR images. Based on the MR imaging and computer post processing parameters, characteristics for the accuracy of thickness determination were derived by a theoretical simulation. The simulated thickness was demonstrated to be well-correlated with the actual in vitro thickness [7]. In 2004, Julio Carballido-Gamio and group discussed the application of NCut with the Nystrom approximation method to segment vertebral bodies from sagittal Tl-weighted magnetic resonance images of the spine [8]. In 2004, Yalin Zheng and group explains about digital videofluoroscopy and it can be used for the study of the motion of spine and it can provide image sequences with many frames, but which often suffer due to noise, exacerbated by the very low radiation dosage [9]. In 2004, V. Grau and group present an improvement to the watershed transform that enables the introduction of prior information in its calculation [10]. In 2004, Meritxell Bach Cuadra and group propose a method for brain atlas deformation in the presence of large space-occupying tumors, based on ana priori model of lesion growth that assumes radial expansion of the lesion from its starting point [11]. In 2004, Albert C. S. Chung and group present an approach to segmenting the brain vasculature in phase contrast magnetic resonance angiography (PC-MRA) [12]. In 2005, Abdolah Chalechale and group present a novel method for image similarity measure, where a hand-drawn rough black and white sketch is compared with an existing data base of full color images [13]. In 2005, Sokratis Makrogiannis and group presented a multiresolution color image segmentation approach that incorporates the main principles of region-based segmentation and cluster-analysis approaches [14]. In 2006, M. Lynch and group developed a novel approach for the automatic segmentation to extract the epi-cardium and endo-cardium boundaries of the left ventricle (lv) of the heart [15]. In 2006, Ying Zhuge and group developed an algorithm for fuzzy-connected image segmentation [16]. In 2006, Ludovic Macaire and group present a new color image segmentation scheme based on unsupervised pixel classification that works even when there is not a one-to-one correspondence between the clusters of color points in the color space and the regions in the image [17]. In 2006, Raz Koren and group propose an automatic detector parameter selection for edge detection which considers both, statistical correspondence of detection results produced from different detector parameters, and spatial correspondence between detected edge points, represented as saliency values [18]. In 2007, Hemg-Hua Chang and group developed a new deformable model, the charged fluid model (CFM), that uses the simulation of a charged fluid to segment anatomic structures in magnetic resonance (MR) images of the brain [19].

2.2 Detection and decision

In 2000, Francois Chabaf and team provided an overview of medical expert systems and to discuss their application to medical imaging, as well future trends in the field [20]. In 2002, Alex P. Zijdenbos and group developed a fully automatic "pipeline" image analysis framework and have successfully applied it to a number of large-scale, multi-center studies (more than 1000 MRI scans) [21]. In 2003, Chuin-Mu Wang and group present a new spectral signature detection approach to magnetic resonance (MR) image classification. It is called constrained energy minimization (CEM) method, which is derived from the minimum variance distortion less response in passive sensor array processing [22]. In 2003, Gholam-Ali Hossein and group proposed a new method for activation detection in event-related functional magnetic resonance imaging (fMRI) [23]. In 2003, Jeffrey Tsao made a study to characterize the artifacts from eight interpolators and to investigate efficient strategies to overcome these artifacts in image registration [24]. In 2003, Gholam-Ali Hossein-Zadeh and team proposed an adaptive spatial filtering method that takes into account contextual information in fMRI activation detection [25]. In 2003, P. Hellier and team propose an evaluation framework, based on global and local measures of the relevance of the registration [26]. In 2004, Xavier Descombes and team were worked with the detection of multiple small brain lesions from magnetic resonance imaging (MRI) data [27]. In 2004, Christopher L. Gilchrist and team investigate the utility of a texture correlation algorithm with first-order displacement mapping terms for use with MR images, and suggest a novel index of image "roughness" as a way to decrease errors associated with the use of texture correlation for intra-tissue strain measurement with MRI [28]. In 2004, Thomas Netsch and team proposed a statistical method for the evaluation of image registration for a series of images based on the assessment of consistency properties of the registration results [29]. In 2005, Chih-Ping Wei and team extended a decision rule induction technique (i.e., CN2 algorithm) to address the challenging characteristics of the targeted learning in radiology [30]. In 2006, Judy R. James and team designed a tool for semi-automated segmentation of the images and calculation of the mismatch volume [31]. With base in object detection and recognition techniques, In 2006, Marcelo Kleber Felisberto and team developed and implemented a new methodology to perform the first head-function of a weld quality interpretation system: the weld bead extraction from a digital radiograph [32]. In 2006, V.S.N. Prasad and team present an approach for whole-body pose-contour matching [33]. In 2007, Celia Varela and team propose a system to detect malignant masses on mammograms [34]. In 2007, Samuel Kadoury and team employed a novel technique, known as locally linear embedding (LLE), for solving the face detection problem [35].

2.3 Filtering and acquisition

In 2002, Wael Badawy and team presented the discrete wavelet transform (DWT), which is one of the most efficient compression algorithms because of its perfect reconstruction property and lack of blocking artifacts [36]. In 2002, Ersin Bayram and team explained about confidence-based anisotropic filtering of magnetic resonance images [37]. In 2003, Aleksandra Pizurica and team proposed a robust wavelet domain method for noise filtering in medical images [38]. In 2003, Temujin Gautama and team introduced a methodology for comparing the nonlinearities present in sets of time series using four different nonlinearity measures, one of which, the "delay vector variance" method, is a novel approach to the characterization of a time series. They did a comparison between BOLD and MION [39]. In 2003, Ralf Mekle and team proposed a new technique to reduce clinical magnetic resonance imaging (MRI) scan time by varying acquisition parameters and sharing k-space data between images [40]. Edge-preserving denoising is of great interest in medical image processing. In 2003, Paul Bao and team presented a wavelet-based multiscale products thresholding scheme for noise suppression of magnetic resonance images [41]. In 2004, Pierre Gravel and team developed a method to study the statistical properties of the noise found in various medical images [42]. In 2006,

Bing Keong Li and team presented and modeled a new method for ameliorating high-field image distortion caused by radio frequency/tissue interaction [43]. In 2006, Victor Taracila and team presented a new method to deal with MRI non-uniformities caused by electromagnetic wave interference patterns at 300-400 MHz in lossy dielectrics [44]. In 2006, Kai-Qi Huang and team proposed a novel color image enhancement method, which is named HVS Controlled Color Image Enhancement and Evaluation algorithm (HCCIEE algorithm) [45].

2.4 Registration and analysis

In 1996, Berkman Sahiner and team developed techniques that use wavelets to perform the localized low-pass filtering for removing the noise present in the high frequencies [46]. To enhance detectability, in 2002, Mukund Desai and Teams work introduces the use of a curve evolution approach that provides separate estimates of the response time shifts at each phase of the stimulus on a pixel-by-pixel basis [47]. In 2002, Dinggang Shen and team presented a new approach referred to as the hierarchical attribute matching mechanism for elastic registration (HAMMER) for elastic registration of medical images, and is applied to magnetic resonance images of the brain [48]. In 2003, T. Hartkens and team quantitatively analyzed the intraoperative brain deformation of 24 subjects to investigate whether simple rules can describe or predict the deformation [49]. In 2003, Thorsten Schormann and team provided a technique [voxel-guided morphometry (VGM)] to quantify macroscopic anatomical differences [50]. In 2003, Kirk W. Finnis and team presented a method of constructing a database of intra-operatively observed human subcortical electrophysiology [51]. In 2003, Bradley P. Sutton and team described a tool for accelerating iterative reconstruction of field-corrected MR images: a novel time-segmented approximation to the MR signal equation [52]. In 2003, Laszlo G. Nyiil and team presented a new class of approaches for rigid-body registration and their evaluation in studying multiple sclerosis (MS) via multiprotocol magnetic resonance imaging (MRI) [53]. In 2003, Julia A. Schnabel and team presented a novel method for validation of nonrigid medical image registration which based on the simulation of physically plausible, biomechanical tissue deformations using finite-element methods [54]. In 2003, Nasser Fatouraee and team introduced a new numerical formulation for improving the accuracy of phase-contrast (PC) velocity fields and corresponding streamlines, based on a physical constraint from fluid dynamics, within a regularization framework [55]. In 2003, Torsten Rohlfing and team extended a previously reported intensity-based nonrigid registration algorithm by using a novel regularization term to constrain the deformation [56]. In 2003, Francois G. Meyer and team explored a new paradigm for the analysis of event-related functional magnetic resonance images (fMRI) of brain activity [57]. In 2003, Josien P. W. Pluim and team presented an overview of the medical image processing literature on mutual-information-based registration [58]. In 2003, James S Duncan and team described the development of the Image Processing and Analysis Group (IPAG) at Yale and the broad range of work in the area of medical image analysis that has been pursued [59]. In 2004, Sea Chen and team presented two novel techniques in order to aid in an improved SNR estimate of the hemodynamic response while preserving statistically significant voxel-wise differences [60]. In 2004, C. Studholme and team examined an alternative approach to separating magnetic resonance imaging (MRI) intensity inhomogeneity from underlying tissue-intensity structure using a direct template-based paradigm [61]. In 2004, Christian F. Beckmann and team presented an integrated approach to probabilistic independent component analysis (ICA) for functional MRI (FMRI) data that allows for nonsquare mixing in the presence of Gaussian noise [62]. In 2004, Mark W. Woolrich and team presented a fully Bayesian approach to modeling in functional magnetic resonance imaging (fMRI), incorporating spatio-temporal noise modeling and hemodynamic response function (HRF) modeling [63]. In 2004, Hamid Soltanian-Zadeh and team presented a fast method for delineation of activated areas of the brain from functional magnetic resonance imaging (fMRI) time series data [64]. In 2004, Alle Meije Wink and team presented a general wavelet-based denoising scheme for

functional magnetic resonance imaging (fMRI) data and compare it to Gaussian smoothing, the traditional denoising method used in fMRI analysis [65]. In 2004, Edward H. Herskovits and team proposed Bayesian morphological analysis methods, based on a Bayesian-network representation, for the analysis of MR brain images [66]. In 2004, J. F. Mangin and team described an alternative object-based strategy dedicated to the cortex. This strategy relies on an artificial neuro anatomist performing automatic recognition of the main cortical sulci and parcellation of the cortical surface into gyral patches [67]. In 2004, Chad W. Washington and team demonstrated successful elasticity image reconstructions in breast cross-sectional images acquired from magnetic resonance (MR) imaging [68]. In 2004, Zhong Xue and team proposed an automatic correspondence detection algorithm for intra modality MR brain images of different subjects using wavelet-based attribute vectors (WAV's) denned on every image voxel [69]. In 2006, Kris Luyten and team showed that how the model-based user interface development methodology can be applied for ambient intelligent environments [70]. . In 2006, Anant Madabhushi and proposed a generalized scale model which is spatially adaptive like other local morphometric models, and yet possesses the global spirit of multi-scale representations [71]. In 2006, Marek'R. Ogiela and team presented a new approach to the interpretation of complex X-ray images, an approach taking advantage of artificial intelligence and soft computing [72]. In 2006, James W. Woods and team described the UMLS Metathesaurus (Meta) concepts to describe medical images [73]. In 2007, Huaien Luo and team proposed a Bayesian approach to analyze the fMRI data with two nonstationary noise models (the time-varying variance noise model and the fractional noise model) [74].

2.5 Technical Development

In 1996, Pascal Haigron and team explained about 3D navigation in Medicine [75]. In 1999, Gilbert R. Hillman and team reported a novel computer method for automatic labeling of structures in 3D MRI data sets using expert anatomical knowledge that is coded in fuzzy sets and fuzzy rules [76]. In 2000, E. Mark Haacke and team pointed out the current image reconstruction and processing issues in MRI for the study of tissue structure and function [77]. In 2000, Ernest V. Garcia and team explained about advances in Nuclear Emission PET and SPECT Imaging [78]. In 2000, Stephen J. Riederer and team explained about current technical development of MRI [79]. In 2000, Robert Turner discussed the biophysics, the MR physics, and the technology underlying the development of functional MRI (fMRI) [80]. In 2004, Theobald O.J. Fuchs and team described the technological basics of multirow detector systems. They discussed the principle aspects of data processing and the resulting image quality for multislice spiral CT (MSCT) systems, which offer rotation speeds up to 2 per second [81]. In 2000, David M. Hansell surveyed the areas of clinical investigation in which variety of image processing techniques were used for the detection of lung abnormalities [82]. In 2000, Peng Wen and team made a study is to develop, through the use of advanced numerical techniques and limited measured data, a new theoretical method to construct head models that include the inherent in-homogeneity of the head tissues and that can be solved numerically [83]. In 2002, Pernilla Selskog and team presented a method for calculation of the time-resolved three-dimensional (3-D) strain-rate tensor using velocity vector information in a 3-D spatial grid during the whole cardiac cycle [84]. In 2002, Jiann-Der Lee and team utilized the patient's computed tomography (CT) data, Schaltenbrand-Wahren (SW) brain atlas, and image processing techniques to develop a novel stereotactic surgical planning system, named Brain Deep Tracer [85]. A novel single-shot trapezoidal-gradient-based Lissajous trajectory is described and implemented on a 3-tesla Magnetic resonance (MR) scanner by Hanhua Feng and team in 2003 [86]. System design and initial phantom accuracy results for a novel biopsy system integrating both magnetic resonance (MR) and ultrasound (US) imaging modalities are presented by C. A. Piron and team in 2003 [87]. Epidaure is the name of a research project launched in 1989 at INRIA, Rocquencourt, close to Paris, France. In 2003, and team explained Medical Image Analysis, Simulation, and Robotics at INRIA [88]. In 2004,

Shigeyuki Suzuki and team developed a virtual surgery system that is capable of simulating surgical maneuvers on elastic organs [89]. In 2005, Mohan Manubhai Trivedi and team presented details of a long-term and ongoing research project on Intelligent environments, where indoor intelligent spaces endowed with a range of useful functionalities are designed, built, and systematically evaluated [90]. In 2006, Dimitra D. Dionysiou and team presented the newest algorithms and simulation results of a computer model of in vivo tumour growth and response to radiotherapy [91]. A combined approach to 3D radial and spiral MRI, COMSPIRA3D (COMbined SPIral and RAdial 3D) was presented by Jose M Perez-Sanchez and team in 2006 [92]. In 2006, Daniel Gareis and team built three transmit-receive phased arrays for ^{1}H, ^{23}Na, and ^{31}P to examine the feasibility of using these arrays at the magnetic field strength of 17.6 Tesla [93]. Data acquisition using a continuously moving table (CMT) is a new method that is capable of generating three-dimensional (3D) large field-of-view (FOV) MR images. Rather than restrict CMT techniques to a constant table translation rate and offline reconstruction, in 2006, M. Sabati and team discussed and implemented a more general real-time approach in which the table motion is decoupled from the MR data acquisition [94]. In 2007, Michael R. Lamprecht and team described the use of the open-source software, CellProfiler™, to automatically identify and measure a variety of biological objects in images [95]. In 2007, Khaled Z. Abd-Elmoniem and team presented an algorithm for the real time myocardium region-of-interest reconstruction and myocardial strain computation using data acquired from a real time pulse sequence [96].

2.6 GUI

In 2002, Stergios Paiamas and team explained about an Internet-Based System for the Commerce of Medical Devices [97]. In 2006, Mark Rossman and team designed an automated algorithm used to analyze SPECT images and provide feedback to users through a visual interface [98]. In 2006, Silvio Antonio Carro and team presented the MedlSeek metadata model that allows one to describe medical visual information (i.e. medical images) of different modalities, including their properties, components, relationships and authorship [99].

The proposed research is a new research topic. Siemens developed some Computer aided diagnosis (CAD), but it is not a complete diagnostic modality. They developed the CAD for Lungs and few specific areas. Siemens also developed some software that can be used for effective handling the slice images.

After having studied various developments that have taken place over the years in the area of medical imaging analysis, MRI techniques and GUI. We started with objectives of extraction of abnormalities in smaller scale and develop algorithms for better image quality of MRI sample.

3. OBJECTIVE

In absence of a well experienced physician, an Intelligent Diagnostic Imaging System (IDIS) can be used to diagnose the abnormalities. It provides the volumetric information of the abnormalities. It will help the surgeon to locate the abnormalities and help to understand the size and severity of the abnormality. The surgeon can plan the surgery in a better manner. This work is very helpful for the entire department especially the Radiology departments of Medical Colleges and Hospitals. No automatic diagnostic imaging system for brain is developed so far. Thus this is very important system. The designed IDIS will have good commercial applications. Precise diagnosis is needed for brain surgery. One of the drawbacks of the present Medical Imaging system is that a well experienced doctor must spend

approximately one hour for diagnosis**.** The designed IDIS and the algorithms developed will avoid these difficulties.

4. DEVELOPMENT OF INTELLIGENT DIAGNOSTIC IMAGING SYSTEM

The important steps for the development of Intelligent Diagnostic Imaging System are

I) Image Preprocessing.

II) Abnormality Extraction (key factor for IDIS).

For abnormality extraction, Different Image segmentation methods are tried. Region growing segmentation algorithm is well suited for abnormality extraction. The threshold detection methods for region growing already available which uses Otsu's method [100] are not working proper for abnormality extraction and it can be applicable only to some of T2 images. Two new algorithms are developed in this work, one for T1 and other for T2. Around 99% of abnormalities of T1 and T2 images can be correctly extracted using the new algorithms.

III) Diagnosis.

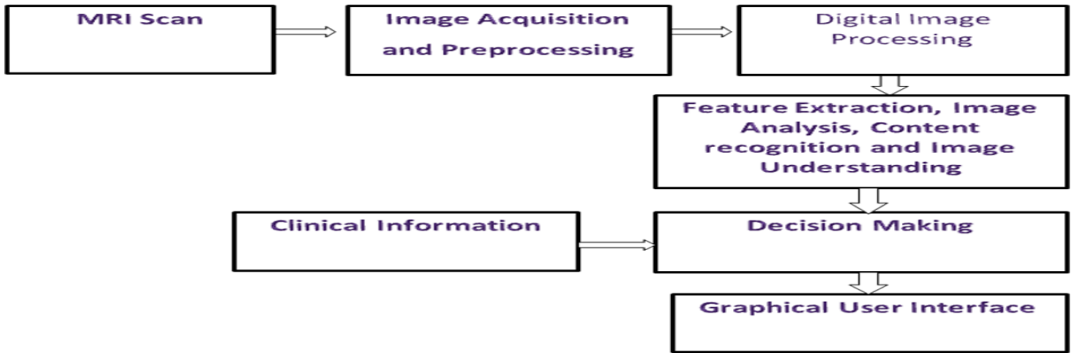

Figure 5: Block Representation of Proposed Intelligent Diagnostic Imaging System.

IV) GUI Development.

MATLAB tools are used for IDIS development.

4.1 Image Processing

The image processing methods that will helps the development of Intelligent Diagnostic Imaging System are Filtering, Restoration, Segmentation, Reconstruction, Registration and Pattern Recognition. Proper filtering methods can be adopted to remove the unwanted signal intensities and motion artifacts [101]. Normally MRI scan sequence lasts for half an hour to two hours. It is very difficult to make the scan without motion artifacts. Because of the patient movement, blur images, overlapped or unclear images may result. One of the options is to repeat the scanning process. If the motion artifact is not severe then image restoration methods can be used [102]. If some abnormalities are found by using image registration or some other means, then from each slice of axial, coronal and sagittal planes, the abnormalities can be segmented and reconstructed to get correct size and shape of abnormalities. Normal slice thickness is 5mm. we count the number of slices in axial, coronal and sagittal direction where the abnormalities are present. Then we multiply the number of slices with the slice thickness in axial, coronal and sagittal direction. This will give volumetric information of the abnormalities. By using the segmented abnormalities from each slice and slice thickness we can reconstruct the abnormalities. This will help the surgeon in

his surgery. The image registration is done on a slice image with same slice image with contrast. This will give clear cut information about the abnormalities present in that slice, if the slice image is abnormal. By using pattern recognition we can recognize whether the abnormality is a tumor or infarction or edema or hemorrhage. It can also be realized whether the tumor is malignant or benign. Benign tumors are well circumscribed tumors.

4.2 Abnormality Extraction

By using image processing methods, it is possible to find the size, shape and thickness of the abnormalities present in the image. Each type of abnormality has its own characteristic. By using these characteristic, the intelligent diagnostic imaging system can realize the abnormalities. T1 and T2 images of same slice are different in terms of intensity level [103]. T1 imaging and T2 imaging are hypo-intensity (hypo) for calcification. T1 is hypo and T2 is hyper-intensity (hyper) for tissue growth. T1 is hypo and T2 is hyper for infarction. If the protein content is more, then T1 is hyper and T2 is hypo. For CSF, T1 is hypo and T2 is hyper [104]. The abnormalities of the brain are due to Intracranial Neoplasm, Cerebral Infections and Inflammations, Stroke, Cerebral Aneurysms, Vascular Malformations, Central Nervous System Trauma and Neurodegenerative Disorders [105]. The Intracranial Neoplasm is concerned with the various Tumors of the nervous system [106]. Some of the Neurodegenerative disorders are Alzheimer's disease, Hydrocephalus, and Pick's disease [107].

So the same identification methodology cannot be applied for these images. A well advanced data base should be created for this intelligent imaging system.

For abnormality Extraction the following segmentation methods are tried

i. Detection of Discontinuities:
Point Detection, Line Detection, Edge Detection & Boundary Detection [108].

ii. Region Based Segmentation:
Region Growing, Region Splitting and Merging [109]

iii. Segmentation by Morphological Watersheds:
Watershed segmentation using the Distance Transformation, Watershed segmentation using Gradients, Marker-Controlled Watershed Segmentation [110].

Among the above segmentation methods, Region growing with the author defined threshold detection algorithm is well suited for abnormality extraction.

4.2.1 Algorithms for threshold detection of T1 and T2 Images

These algorithms are developed by the author.

- Different algorithms for T1 and T2 Images.
- Threshold is based on the analysis of the histogram and represents

i) The difference between 255 and the location of the valley point decided by the algorithm for T2.

ii) The difference between 0 and the location of the valley point decided by the algorithm for T1.

• Histogram is divided into many overlapped subsections. Find the maxima of each subsection. For that a moving window is used of size 10 and it is moved from high intensity level to the low intensity level for T1 and T2 in an overlapped manner of 5 intensity level and finds the maxima (pixel). In this algorithm size of the subsection is 10 intensity levels.

• For T2, the maxima values are analyzed from high intensity side to the low intensity side. For T1 it is vice versa. For T2 the first hill point can be found by the following method. If three consecutive maxima are identical in high intensity side, then that maxima is considered as hill point or if two consecutive maxima values are identical and left and right maxima from the identical maxima are decreasing in magnitude in high intensity side then the identical maxima whose intensity levels are same can be consider as a hill point. The first hill point can be found by the following MATLAB sub-program.

```
for j=1:1:44
     if(((M(j)==M(j+1))&(M(j)==M(j+2)))|  (M(j)==M(j+1)))&((((M(j)-M(j-
1))>0)|((M(j-1)-M(j-2))>0))&(((M(j)-M(j-1))>=0)|((M(j-1)-M(j-2))>=0)))
&((((M(j+1)-M(j+2))>0)|((M(j+2)-M(j+3))>0))&(((M(j+1)-M(j+2))>=0)|((M(j+2)-
M(j+3))>=0)))))
                e=j+4; T1=M(j); k1=I(j);
                break;
             end;
            end;
```

where M(j) s are the maxima values, T1 is the first hill point. k1 is the corresponding intensity value.

The first candidates for the second hill point can be found by the following subprogram.

```
T2=0; k2=0;
        if e<45
        for q=e:1:44
          if  (M(q)==M(q+1))&((((M(q)-M(q-1))>0)|((M(q-1)-M(q-
2))>0))&(((M(q)-M(q-1))>=0)|((M(q-1)-M(q-2))>=0)))&((((M(q+1)-
M(q+2))>0)|((M(q+2)-M(q+3))>0))&(((M(q+1)-M(q+2))>=0)|((M(q+2)-
M(q+3))>=0)))
               h=q+2; T2=M(q);  k2=I(q);
                break;
             end;
            end;
         end;
```

where M(q)s are the maxima values, T2 is the candidate for the second hill point. k2 is the corresponding intensity value.

Similarly the second candidate for the second hill point also can be found.

• From the candidates we have to find the second hill point. Following subprogram can be used for that purpose.

```
if ((T3>T2)|(abs(T3-T2)<500))&((k1-k3)<175)
        Th=T3;kh=k3;
        elseif (T2==0)&(T3==0)
                mx=0;
                if e<47
                for p=e:1:47
                    if M(p)>mx
                        mx=M(p);
                     end;
                end;
```

```
            for p=e:1:47
        if M(p)==mx
            Th=M(p);kh=I(p);
    break;
    end; end; end;
    else
        Th=T2;  kh=k2;
             end;
```

Where Th is the second hill point, kh is the corresponding intensity value, T2 and T3 are the candidates for the second hill point. M(p) is the maxima and I(p) is the corresponding intensity value.

- The space between the two hill point is divided into three region and finding the valley point of each section. If all the valley points satisfy a predefined criteria then left most valley point is considered for T2 as main valley point and rightmost valley point is considered for T1.

```
if ((abs(min3-min1))<400)&((abs(min3-min2))<400)
          d=d3;
       elseif ((abs(min2-min1))<400)&((abs(min2-min3))<400)  d=d2;
         elseif (min2<min1)  d=d2;
       elseif (min1<min2) d=d1;
       end;
        else
            min=T1;
       for i=k1:-1:kh
           if h1(i)< min
               min=h1(i);
           end; end;
       for i=k1:-1:kh
           if h1(i)==min
               d=i;
               break;   end; end;   end;
```

- Absolute value of the subtraction of main valley point from the Seed Point gives the threshold.

- Seed Point can be decided by the author. Seed Point can be a single point or a matrix. In IDIS Seed Point is a single point and it is the maximum intensity point for T2 images and minimum intensity point for T1 images.

4.2.2 Region Growing

It is a procedure that groups pixels or sub regions into larger regions based on predefined criteria for growth. The basic approach is to start with a set of "seed" points and from these grow regions by appending to each seed those neighboring pixels that have predefined properties similar to the seed.

The MATLAB M function regiongrow is used for the segmentation [111].

The syntax for this function is

[G, NR, SI, TI] = regiongrow(F, S, T)

Input F is the slice image from which we have to extract the abnormalities. S can be an array (same size as F) with a 1 at the coordinates of every seed point and 0s elsewhere. S can also be a single seed value. T can be an array (the same size as F) containing a threshold value

for each pixel in F. T can also be a scalar, in which case it becomes a global threshold. Output G is the result of region growing, with each region labeled by a different integer. NR is the number of regions. SI is the final seed image used by the algorithm. TI is the image consisting of the pixels in F that satisfies the threshold test [112]. By checking various output images, it is found that T1 is the desired abnormality extracted image.

Input S is the seedpoint and it is a scalar whose value is equal to the highest intensity level of the image. The value of the S is found by using author defined MATLAB M function ***seedpo*.**

S=*seedpo*(F)

Input F is the slice image from that we have to extract the abnormalities.

Input T is a scalar, whose value is found by using author defined MATLAB M function ***threshodep_modt1*** for T1 images and ***threshodep_modt2*** for T2 images. These functions use the threshold detection algorithm developed by the author.

T= *threshodep_modt1* (F,S) for T1

or

T= ***threshodep_modt2(F,S)*** for T2

Input S is the output of ***seedpo.*** Input F is the slice image from that we have to extract the abnormalities**.**

T can also be found by ***graythresh*** MATLAB M function. But by using the ***graythresh,*** only a few abnormality extractions can be done from T2 images. It fails completely for T1 images.

4.2.3 Region Growing Abnormality Extraction Result Comparison

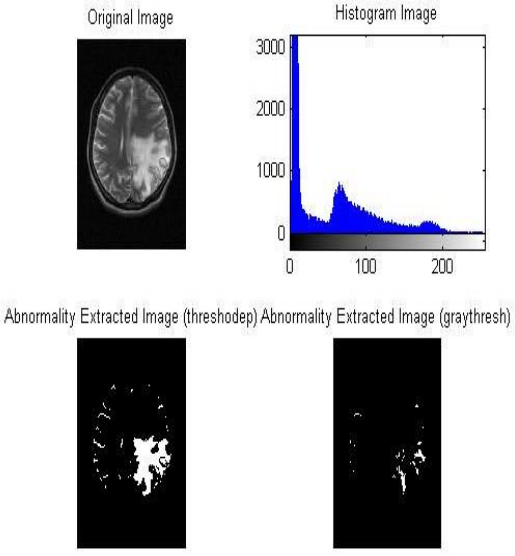

Figure 6. T2 Turbo Spin-echo Axial 13th Slice Image of a 30 year old patient with Venous Infarct. Extraction using regional growing segmentation algorithm with threshodep_modt2 and graythresh function. Function threshodep_modt2 gives perfect result and graythresh failed in this case.

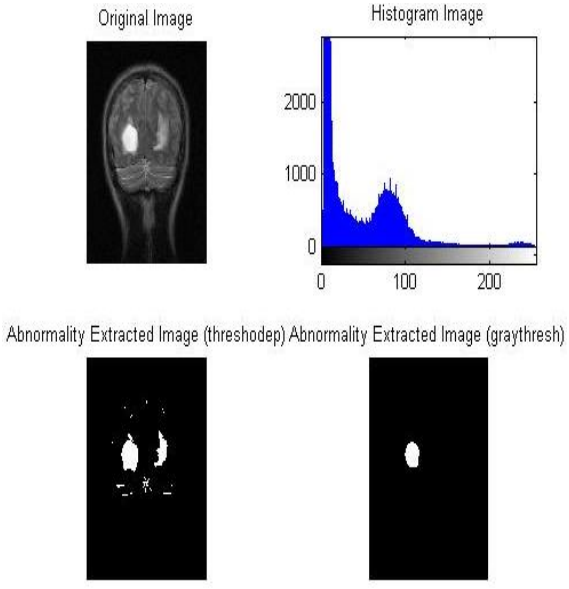

Figure.7. T2 Turbo Spin-echo Coronal 18th Slice Image of a 18 year old patient with hydrocephalus due to Colloid Cyst. Extraction using regional growing segmentation algorithm with threshodep_modt2 and graythresh function. Function threshodep_modt2 gives better result compared to graythresh.

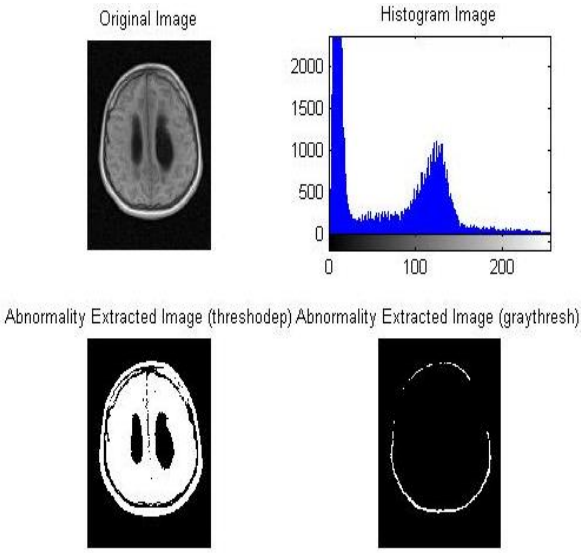

Figure 8. T1 Spin-echo Axial 15 th Slice Image of a 18 year old patient with hydrocephalus due to Colloid Cyst. Extraction using regional growing segmentation algorithm with threshodep_modt1 and graythresh function. Function graythresh failed in this case.

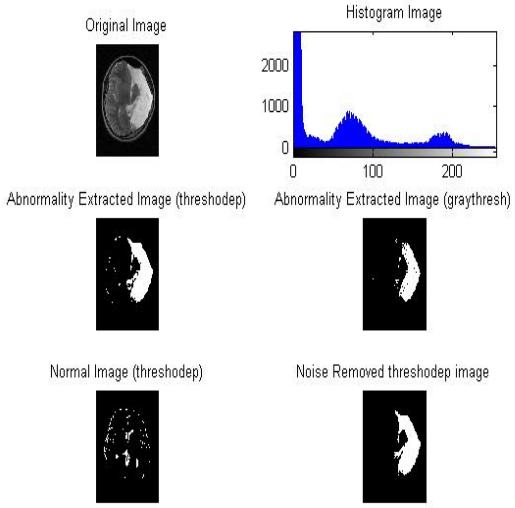

Figure 9. T2 Turbo-Spin-echo Axial 10 th Slice Image of a 16 year old patient with hemorrhage. Extraction using regional growing segmentation algorithm with threshodep_modt2 and graythresh function. Same slice image of a normal patient of same age group using regional growing segmentation algorithm with threshodep_modt2 Function. Noise removed image also shown.

4.2.4 Region Splitting and Merging

Subdivide an image initially into a set of arbitrary, disjointed regions and then merge and/or split the regions in an attempt to satisfy the conditions stated by the predicate P. The MATLAB M function ***splitmerge*** is formed and used to do Region Splitting and Merging segmentation.

G=*splitmerge*(F, mindim, @predicate)

Input F is the slice image from which we have to extract the abnormalities. **mindim** specifies the minimum dimension of the subimages (a positive integer power of 2). **predicate** is a author defined function which sets flag to TRUE if intensities of the pixel in the region have a standard deviation that exceeds 9 and their mean intensity is between 0 and 255.

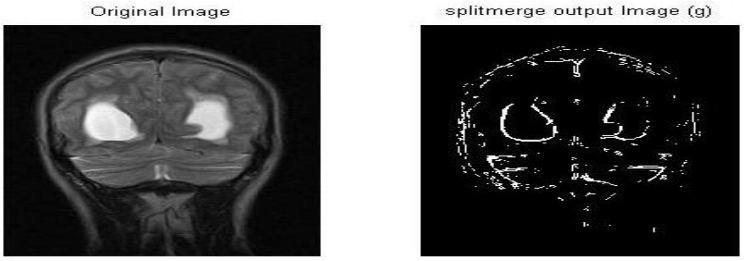

Figure 10. T2 Turbo Spin-echo Coronal 19th Slice Image. Extraction using *splitmerge* MATLAB M function. predicate is an argument of *splitmerge* function and it is a author defined function sets flag to TRUE if intensities of the pixel in the region have a standard deviation that exceeds 9 and their mean intensity is between 0 and 255.

4.2.5 Marker-Controlled Watershed Segmentation

Direct application of the watershed transform to a gradient image usually leads to over-segmentation due to noise and other local irregularities of the gradient. Over-segmentation can be controlled based on the concept of markers. A marker is a connected component belonging to an image [113].

The MATLAB functions with syntax to set the internal markers and watershed transform are **Im=imextendedmin(f, 2); fim=f; fim(im)=175;**

Lm=watershed(bwdist(im)); em=Lim==0;

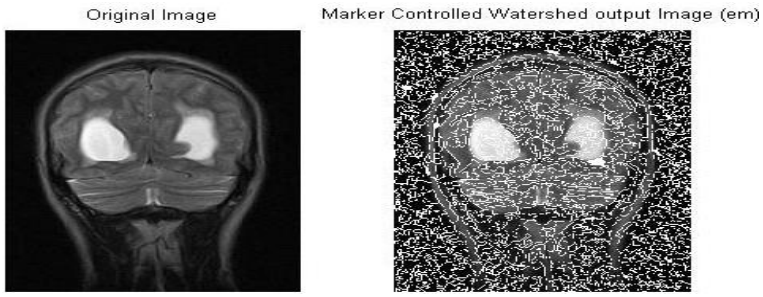

Figure11. T2 Turbo Spin-echo Coronal 19th Slice Image with Marker-Controlled Watershed Segmentation

5. SPECIFICITY/SENSITIVITY/ACCURACY TABLE OF ABNORMALITY EXTRACTION

S.L No	Abnor-mality	No of Patients	Mode & Slice Mode	Total number of abnormality slices	Abnormality extraction	Accuracy (Individual Slices)	Accuracy (overall)	Diagnosis Sensitivity
1	Hydroc-ephalus	3	T1 Axial	34	threshodep_modt1 (Author defined)	99%	93%	96%
					Graythresh (Otsu Method)	0%	0%	
			T2 Coronal	36	threshodep_modt2 (Author defined)	99%	92%	96%
					Graythresh (Otsu Method)	40%	30%	
2	Infract-ion	4	T1 Sagittal	62	threshodep_modt1 (Author defined)	99%	90%	96%
					Graythresh (Otsu Method)	0%	0%	
			T2 Axial	58	threshodep_modt2 (Author defined)	99%	91%	96%
					Graythresh (Otsu Method)	30%	28%	
3	Benign Tumors	1	T1 Coronal	12	threshodep_modt1 (Author defined)	99%	93%	96%
					Graythresh (Otsu Method)	0%	0%	
			T2 Coronal	12	threshodep_modt2 (Author defined)	99%	93%	96%
					Graythresh (Otsu Method)	40%	36%	

Table 1: Table compares the accuracy of author defined method with existing Otsu method for a few brain abnormalities. It also shows the diagnosis sensitivity. The result is almost same for other abnormalities also.

6. COMPARISON RESULT OF DIFFERENT ABNORMALITY EXTRACTION METHODS

- After working with many samples, it is found that using Region Growing Segmentation algorithm with automatic seed point and author defined threshold functions, the abnormalities are precisely extracted.
- Author defined functions *threshodep_modt1* and *threshodep_modt2* succeeded about 99% of cases
- *graythresh* MATLAB M function succeeded only for 30 to 40 percentage of cases of T2 images only. g*raythresh* failed in T1 images.
- If the image contains hypo and hyper intensity abnormalities then both algorithms *threshodep_modt1* and *threshodep_modt2* should be used to extract the abnormalities.
- Abnormality extraction using Region Splitting and Merging Segmentation algorithm with the function predicate is not up to the level.
- The extraction of the abnormalities using the Marker Controlled Watershed Segmentation is also not giving good results.

7. ABNORMALITIES EXTRACTED BY THE ALGORITHM

All the abnormalities with clear intensity change can be detected by the algorithm. Benign Tumors, Malignant Tumors, Hydrocephalus and Different type Lesions can be detected by the algorithm developed in this work. If the abnormality is hyper intensity in nature then *threshodep_modt2* function or algorithm for T2 is used for abnormality extraction. If the abnormality is hypo intensity in nature then *threshodep_modt1* function or algorithm for T1 is used for abnormality extraction. If the abnormality contain hyper intensity and hypo intensity region then both algorithm must used for abnormality extraction.

8. DEVELOPMENT OF GUI

In the GUI for IDIS, edit boxes, popup menus, push button etc are developed to help the user for the easy operation of GUI. The patient name and file path are entered through the edit boxes [114]. Modality (T1 fl3d, T1 se, T2 tse etc) is selected by a popup menu. Slice mode (Axial, Sagittal, Coronal etc) and Slice number are also selected through popup menu. Severity of abnormality can be understood in this GUI by comparing the abnormality image with same age group, same modality, same slice mode and same slice number of a normal person. The *abextract* pushbutton callback (subroutines) comprises of the regional growing segmentation algorithm with automatic seed point and threshold detection is used for extracting the abnormalities of the MRI Images. Threshold detection is done by using author defined *threshodep_modt1* or *threshodep_modt2* function and *graythresh* MATLAB M function. Comparison of author defined *threshodep_modt1* or *threshodep_modt2* function and *graythresh* MATLAB M function can also be done on GUI.

Another important part of the GUI is the Diagnostic facility. By pressing the Diagnosis button, the system will diagnose the abnormality. There is provision for reset the system also in the form of Reset button.

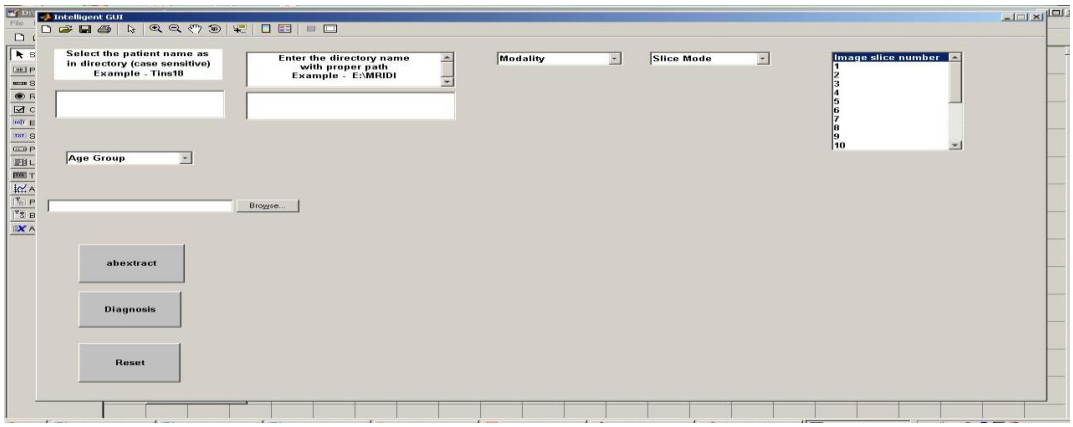

Figure12. GUI front plane

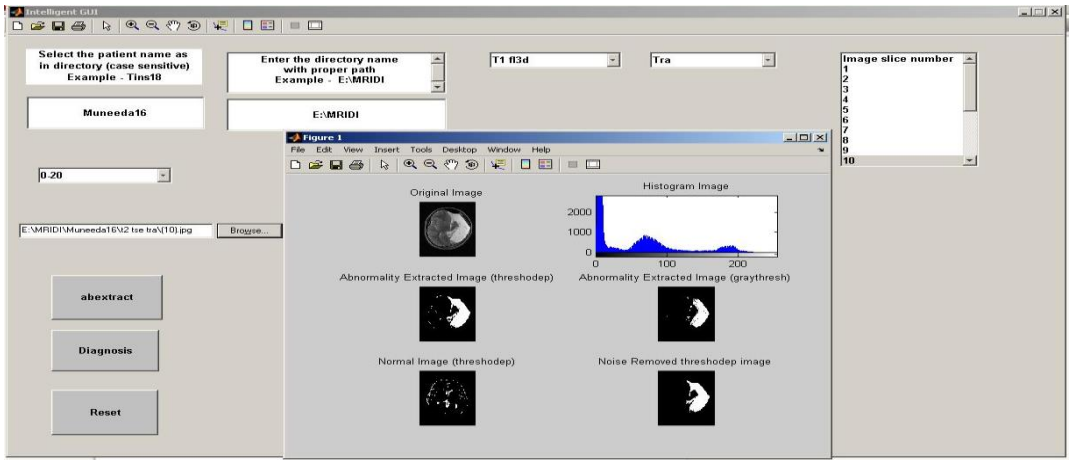

Figure13. GUI with abextract button is pressed.

9. DIAGNOSIS

After the abnormality extraction, the abnormality extracted images must be processed as follows for diagnosis.

- a) Filtering (abnormality extracted image)
- b) Intensity to Binary Image Conversion
- c) Noise removal
- d) Boundary calculation
- e) Area calculation
- f) Perimeter calculation
- g) Metric calculation
- h) Decision Making

Depending on the Metric Value we can do the diagnosis

Eg: If Metric >0.90 then it is Benign Tumors

If Metric <0.90 & >0.75 then it is Malignant Tumors

If Metric <0.75 & >0.30 then it is Hydrocephalus

If Metric <0.30 then it is Lesion (Hemorrhage, Infarction)

Metric calculation of all abnormality slices of a particular patient must be done prior to the decision making. The range of Metric of majority of the slices must be considered for decision making.

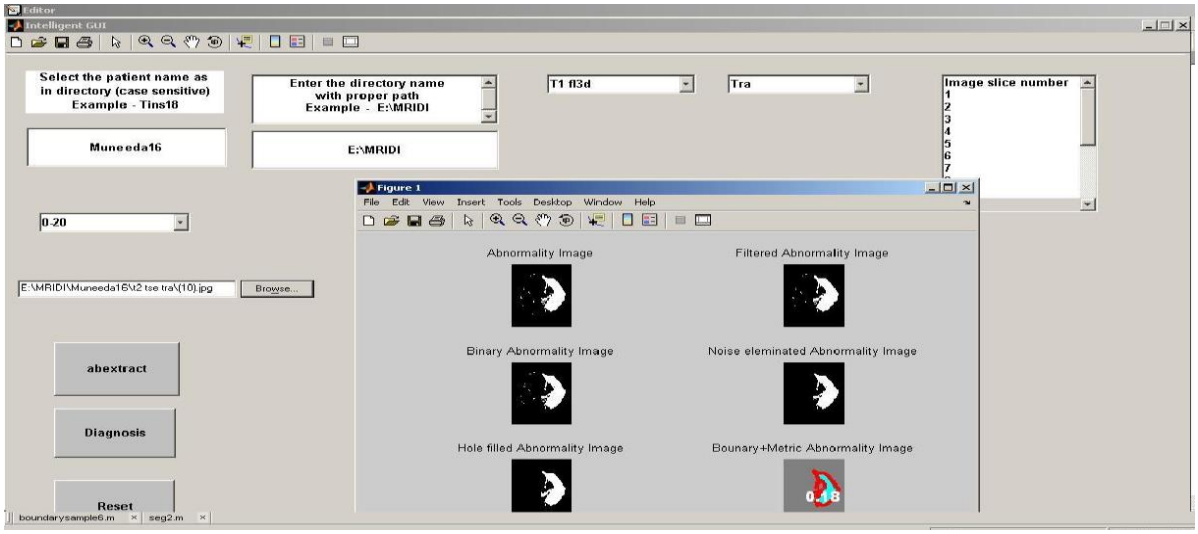

Figure14. GUI with Diagnosis button is pressed. In the above diagram the metric value is 0.18 so the abnormality is due to lesion.

10. CLINICAL STUDY WITH DOCTORS REPORT AND IDIS RESULT

Many MRI samples of different patients were taken and studied. The developed algorithm was applied to find abnormalities and structural studies were done for diagnosis. Few of which are explained as follows.

10.1 Case 1

Report No: 602275, Patient No :715554, Sex :Male, Age : 17 , Date: 25-07-2008, Patient name: Tins

10.1.1 Symptoms

Irritability, headache, sleepiness, vomiting, personality and memory changes, difficulty walking, and urinary incontinence

10.1.2 Scanning Result

MRI head plain and contrast was performed using T1W, T2W, FLAIR sequences in various planes. Lateral ventricles are grossly dilated with peri ventricular seepage. 3rd and 4th ventricle appears normal. Evidence of rounded altered signal intensity lesion at the foramen of monro in the roof of 3rd ventricle measuring 17X17 mm. Lesion is isointense in TlWI, briqht in FLAIR and mildly hyperintense in T2W. Post contrast scan shows peripheral rim enhancement. Supratentorial neuroparenchyma appears normal in siqnal intensity. No focal lesions noted. Basal qanqlia, internal capsule, Thalami are normal in size and siqnal intensity. Posterior fossa structures including cerebellum, medul1a, pons, midbrain appear normal in signal intensity. No midline shift. No evidence of sellar/para sellar mass lesion noted. The signal void of cerebral vessels in the region of circle of willis and dural venous sinuses are normal. Visualized orbit appear normal.

10.1.3 Impression: MR features shows, round, altered signal intensity lesion at the foramen of monro level with obstructive hydrocephalus.

10.1.4 Possibility: colloid cyst (benign congenital tumors).

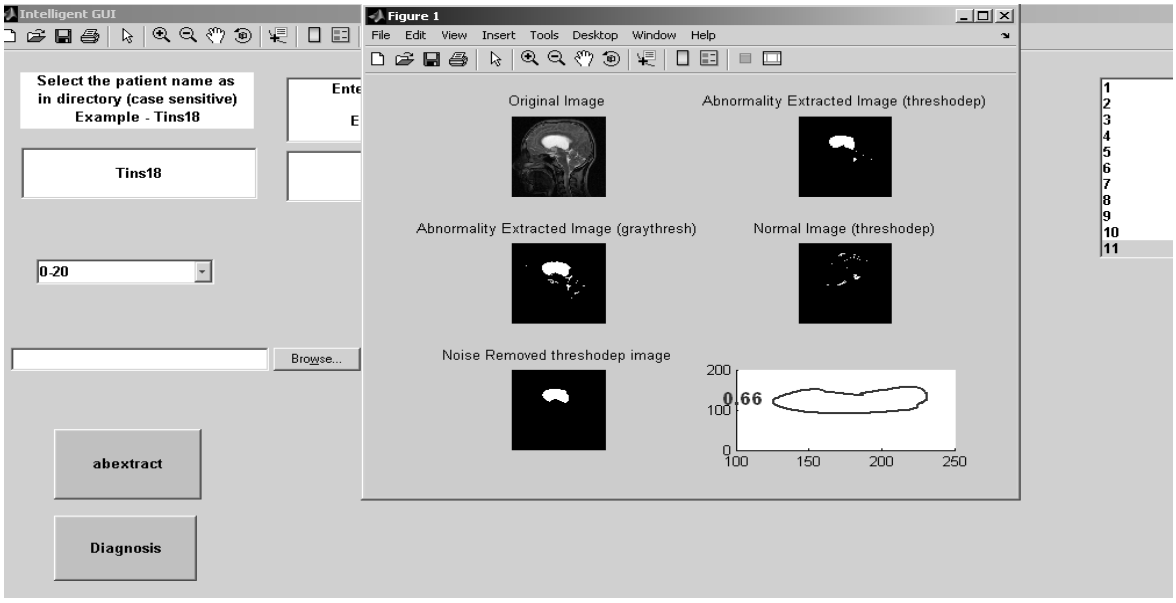

Figure15 a.

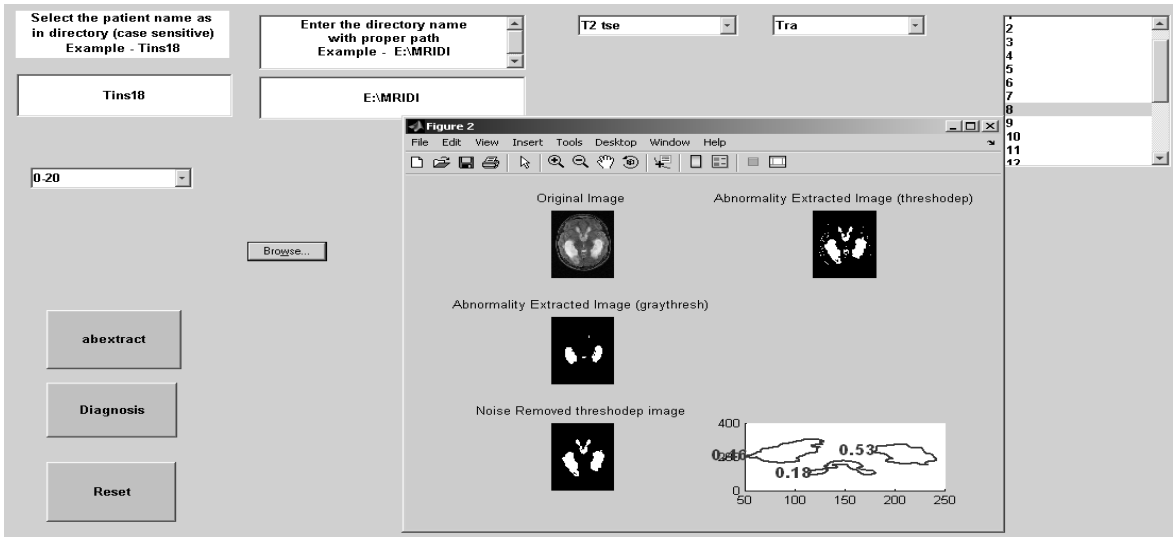

Figure 15 b.

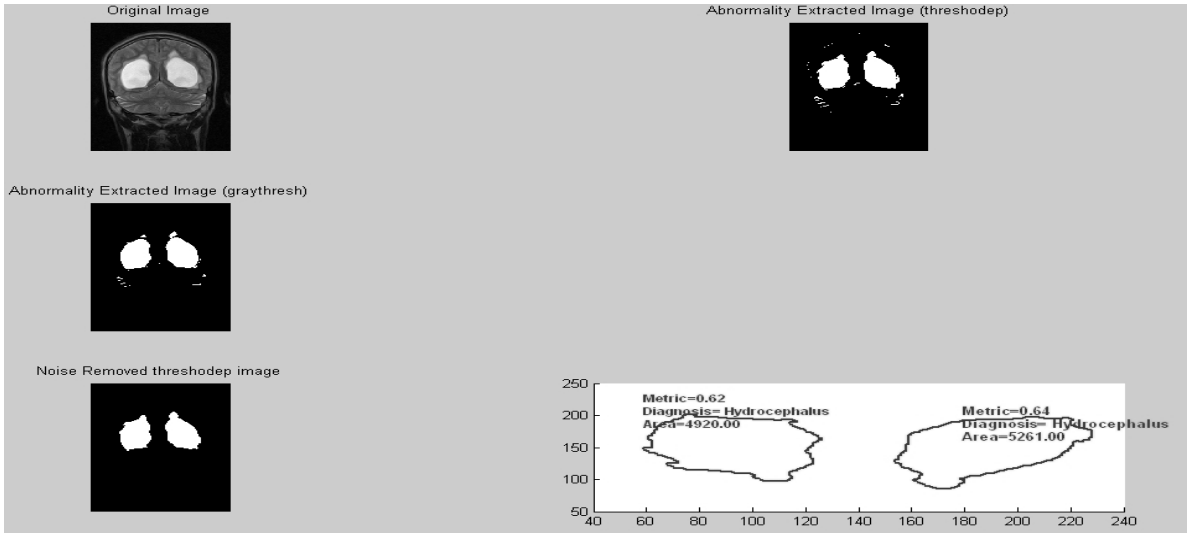

Figure 15 c

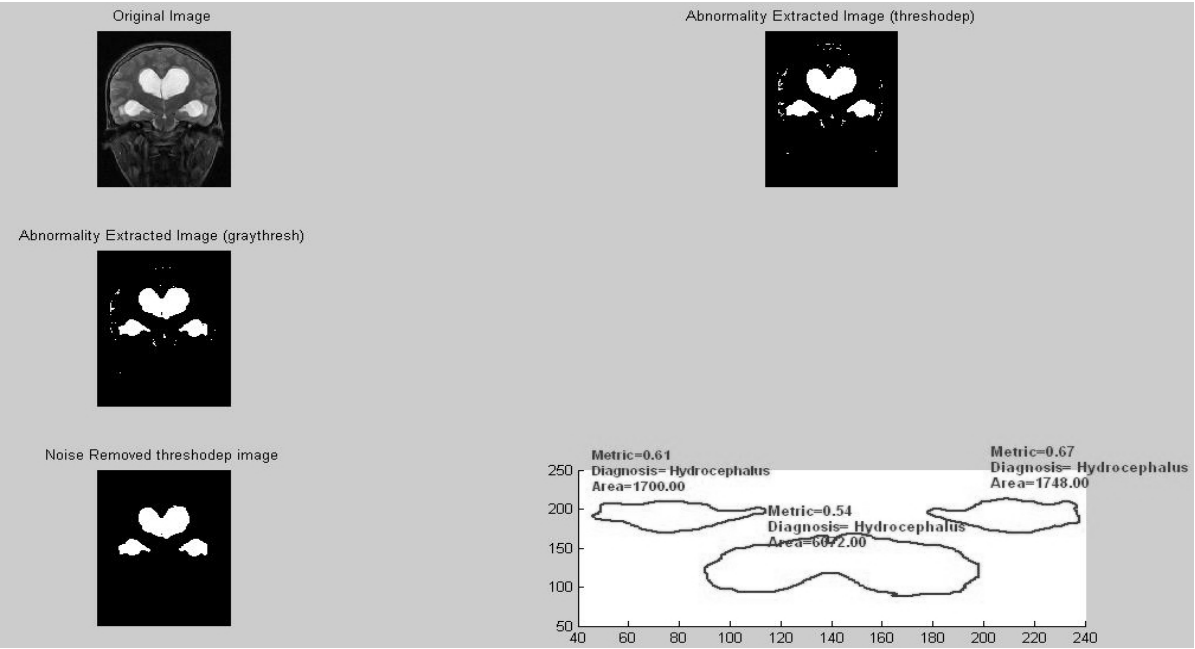

Figure 15 d
Figure 15 a-d IDIS Result on different slice images of patient in case 1 which matches doctors finding.

10.2 Case 2

Report No : 602409, Patient No : 714275,Sex : Female,
Age : 32 , Date :30-08-2008, Patient name: Nafeesa

10.2.1Symptoms

Headaches, Neck pain or stiffness, Nausea, vomiting, and lack of appetite, Vision changes or eye pain, changes in mood, personality, behavior, mental ability, and concentration, Memory loss or confusion, Seizures, Fever, Difficulty moving

10.2.2 Scanning Result

MRI head plain was performed using T1W, T2W, FLAIR Post contrast T1W sequences in various planes. A focal altered signal intensity lesion seen in left parietal deep white matter. The lesion is hypointense on Tl and Flair and hyper on T2WI. There is evidence of perilesional edema in surrounding white matter which is hypo on Tl and hyper on T2 and FLAIR. No evidence of significant mass effect. Following IV contrast, two closely related ring enhancing lesions are seen within this altered signal intensity area. Basal qanglia, internal capsule, Thaiami are normal in size and signal intensity. Posterior fossa structures including cerebe1lum,medul1a, pons, midbrain appear normal in signal intensity. No midline shift. No evidence of sellar/para sellar mass lesion noted. Ventricles and basal cisterns are normal. No hydrocephalus noted. The signal void of cerebral vessels in the region of circle of willis and dural venous sinuses are normal. Visualized orbit appear normal.

10.2.3 Impression : altered signal intensity lesion in left partial deep white matter hypointense on T1 and FLAIR and hyper on T2 with perilesional edema and showing ring enhancement following IV contrast. Findings suggestive of granulomatous lesion

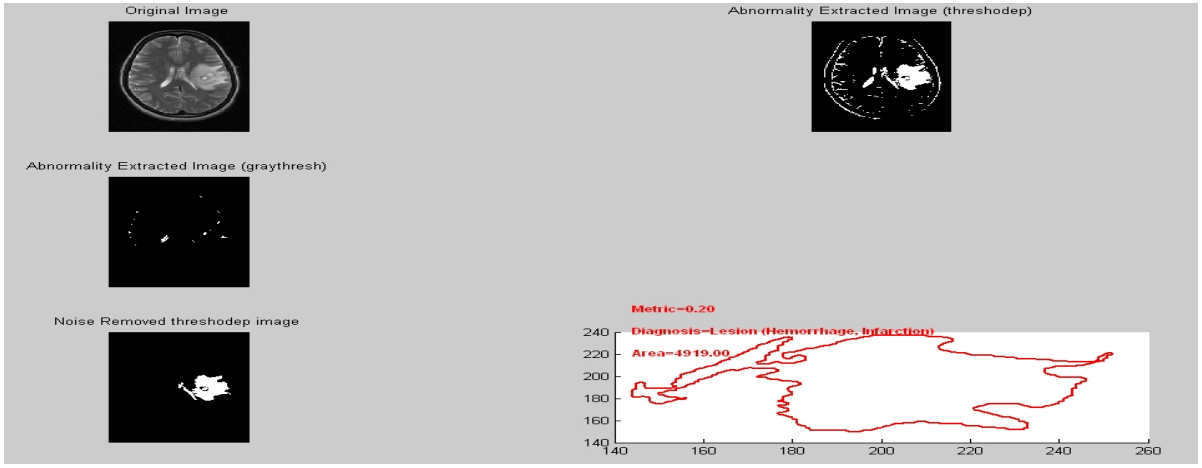

Figure 16a

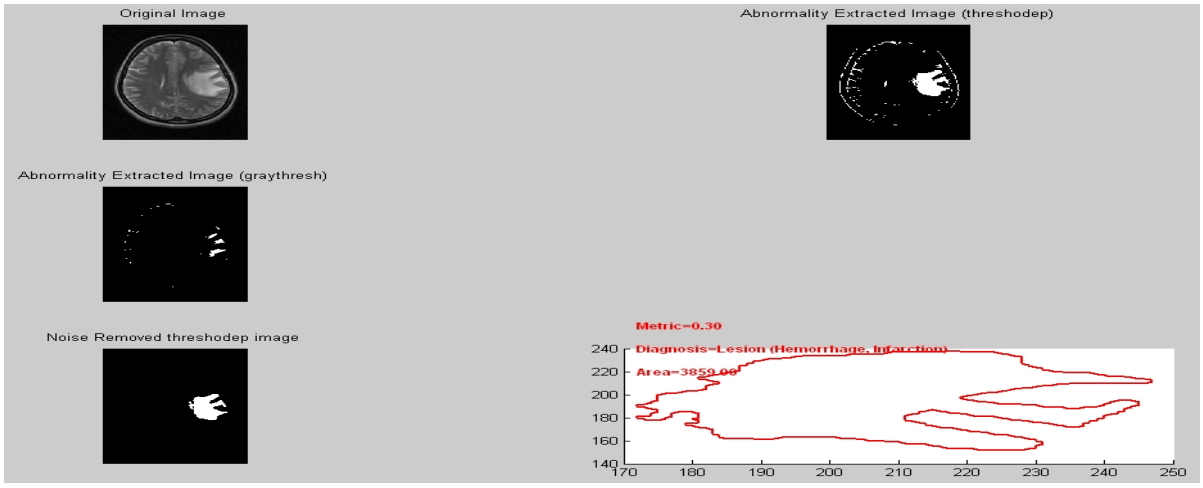

Figure 16b
Figure 16 a, b, IDIS Result on different slice images of patient in case 2 which matches doctors finding.

10.3 Case 3

Report No: 602338 , Patient No: 484844, Sex: Male, Age :53 Date :12-08-2008,Patient name: Damodhar Salian

10.3.1 Symptoms

On the opposite side of the body there are loss of sensations and weakness. Physical examination of the head area revealed abnormal pupil dilation, light reaction and lack of eye movement on opposite side. The infarction occurs on the left side brain, so speech will be slurred and reflexes aggravated as well.

10.3.2 Scanning Result

MRI head plain was performed using T1W,T2W,FLAIR sequences in various planes. Altered signal intensity lesion noted in the left cerebellar cortex and left fronto parietal cortex. Lesion appears hypo in T1WI, FLAIR, hyper in T2WI. No mass effect. No perilesional edema. Prominent cerebral sulci, cisternal spaces noted. Supratentorial neuroparenchyma appears normal in signal intensity. No focal lesions noted. Basal ganglia, internal capsule,

Thalami are normal in size and signal intensity. Posterioensr fossa structures including medulla, pons, midbrain appear normal in signal intensity. No midline shift. No evidence of seller/para sellar mass lesion noted.Ventricles and basal cisterns are normal. No hydrocephalus noted. The signal void of cerebral vessels in the region of circle of willis and dural venous sinuses are normal. Visualized orbit appear normal.

10.3.3 Impression: MR features shows, altered signal intensity lesion in the left cerebellar and fronto parietal cortex. Sign of subacute/chronic infarcts, cortical atrophic changes.

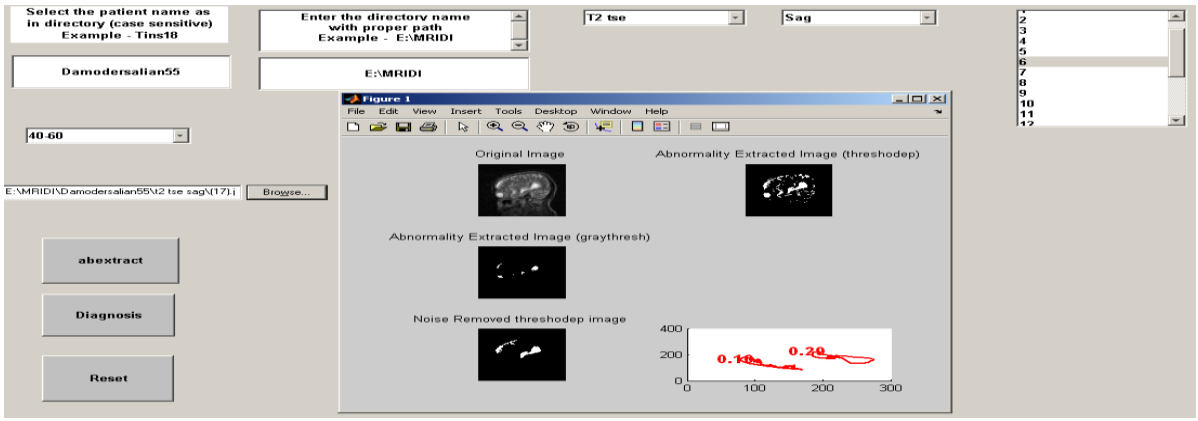

Figure 17 a

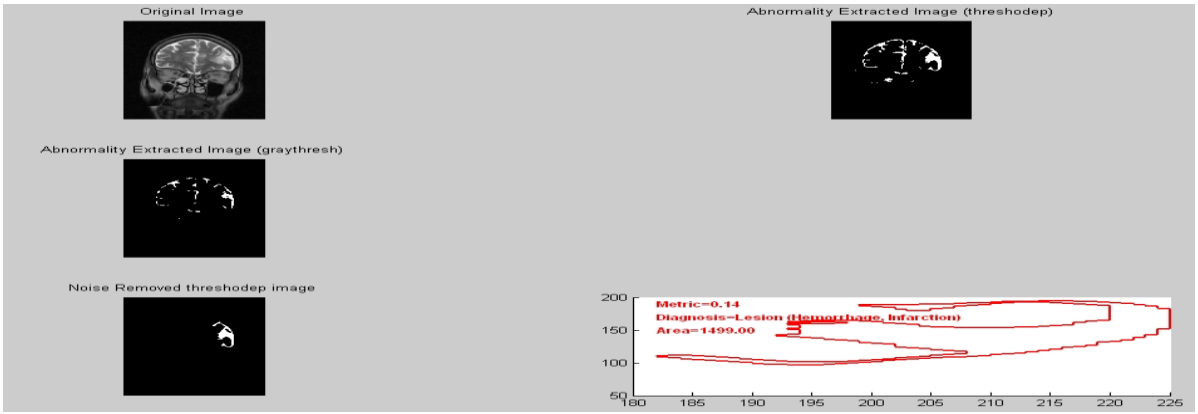

Figure 17b

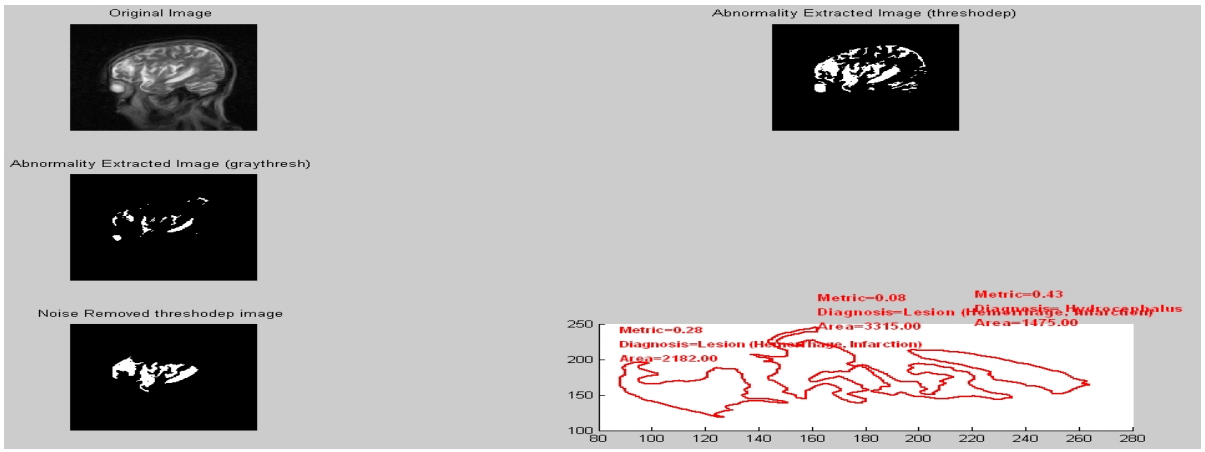

Figure 17c

Figure 17 a, b, c, IDIS Result on different slice images of patient in case 3 which matches doctors finding

10.4 Case 4

Report No: 602290, Patient No: 483096, Sex : Male, Age: 46, Date :30-07-2008, Patient name: Mohanan

10.4.1 Symptoms

Ipsilateral sensorineural hearing loss/deafness, disturbed sense of balance and altered gait, vertigo with associated nausea and vomiting, pressure in the ear, and tinnitus (most often a unilateral high-pitched ringing, sometimes a machinery-like roaring or hissing sound, like a steam kettle).

10.4.2 Scanning Result

MRI head plain and contrast was performed using T1W, T2W, FLAIR and Post contrast T1W sequences in various planes. Evidence of well circumscribed extraaxial altered siqnal intensity lesion in the left cerebello pontine angle measuring 3.23X2.93cm.Lesion is hypo in T1WI, mildily hyperintense in T2WI and FLAIR. Peri1esional edema noted with mass effect compressing the 4th ventricle. Brain stem rotation noted. Buckling of cerebellar white matter noted. Post contrast study shows intense homogeneous enhancement. No signal void/calcification. Lateral and 3rd ventricles are mildly dilated. Intracanalicular extension not appreciated. Rest of the tarain parenchyma normal. Basal qanglia, internal capsule, Thalami are normal in size and signal intensity Posterior fossa structures includinq pons, midbrain appear normal in signal intensity. No midline shift. No evidence of sellar/para sellar mass lesion noted. The signal void of cerebral vessels in the region of circle of willis and dural venous sinuses are normal. Visualized orbit appear normal.

10.4.3 Impression : MR features shows, Well circumscribed, intense homogenously enhancing extra axial mass lesion in the left cerebllo pontine angle with perilesional edema compressing the brain stem and 4th ventricle.

10.4.4 Possibility: Acoustic Schwannomma (Benign growths- intracranial tumor of the myelin-forming cells of the vestibulocochlear nerve)

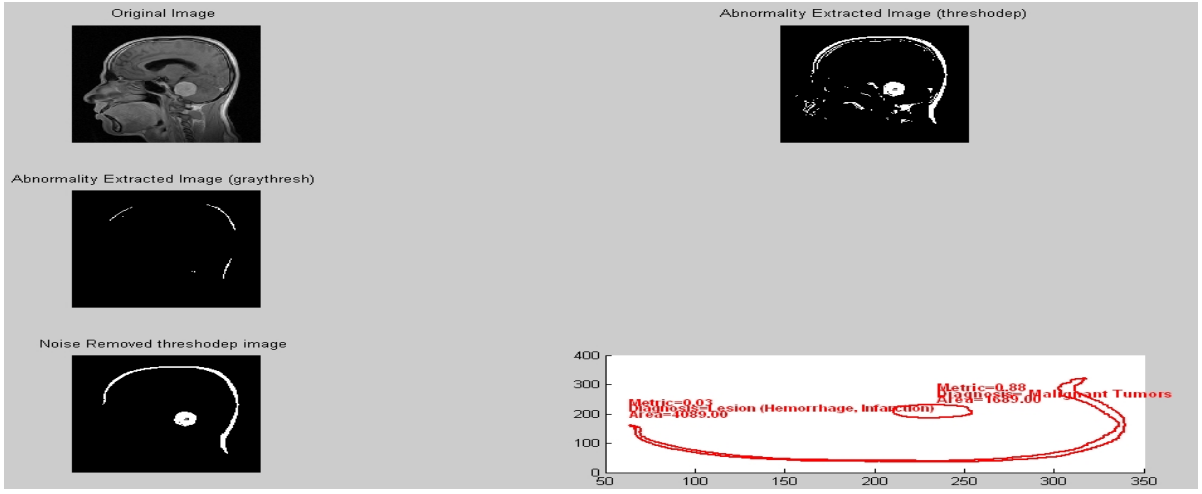

Figure 18 a, IDIS Result on different slice images of patient in case 2 which matches doctors finding

11 RESULTS

It is found that the algorithm detects the abnormalities and the structural studies go with the diagnosis by the doctor. Thus clinical findings with doctors report matches with the conclusion of the developed work.

12. ABNORMALITIES DIAGNOSED BY THE ALGORITHM

All the major abnormalities with clear intensity change can be diagnosed by the algorithm. Benign Tumors, Malignant Tumors, Hydrocephalus and Different type Lesions can be diagnosed by the algorithm developed in this work.

13. ADVANTAGES OF THE ALGORITHM IN TERMS OF AMOUNT AND EASE OF COMPUTATION

This algorithm uses very simple technique for its development. It is developed from the very basic topology and it can be easily implemented using almost all software. Abnormality extraction needs more computation time but diagnosis part can be easily done. It can also be easily embedded into MRI machine peripherals.

14. OVERALL RESULTS AND SCOPE FOR FUTURE WORK

Intelligent Algorithms are developed for Diagnosis of Brain Abnormalities and Diseases from MRI Images. In this work a threshold detection algorithm is developed to facilitate precise abnormality extraction using region growing segmentation. Once the perfect abnormality extraction is done, it is shown that diagnosis can be done using metric calculation of all the slices of abnormality images of a particular patient.

Present Algorithm can be used for the diagnosis of major abnormalities with clear intensity change. There are lots of abnormalities where the intensity change is not evident. Therefore technologies can be developed so that the system can be a complete diagnostic system. More features that can even detect the complicated diseases like Alzheimer's disease can be added to the system. All slice abnormalities of a particular patient can be assembled to get volumetric information of the abnormalities which will help the surgeon while performing surgery.

Dr. A. M. Khan **Jose Alex Mathew**

(Research Guide) **(Candidate)**

Publications- International

1. Jose Alex Mathew, A.M.Khan, U.C. Niranjan, "Digital Image Processing Methods to find the Abnormalities of the Brain for the Development of Intelligent Diagnostic Imaging System", International Journal of Computational Intelligence Research and Applications. ISSN: 0973-6794, Vol.3, 2009, pp. 169-174.

2. Jose Alex Mathew, A.M.Khan, U.C. Niranjan, "Image Segmentation and Classification of the MRI Images to find the Abnormalities of the Brain for the Development of an Intelligent Diagnostic Imaging System", Publised in Narosa Publications.

3. Jose Alex Mathew, A.M.Khan, U.C. Niranjan, "Algorithms to find the thresholds for the Abnormality Extraction of the MRI slice Images of a GUI based Intelligent Diagnostic Imaging System", This paper is published as a special Issue in International Journal of Computer Applications (IJCA) with ISBN: 978-93-80746-57-8. This issues will be Indexed with DOAJ, Google Scholar, Informatics, ProQuest CSA Technology Research Database, ScientificCommons Index and Georgetown University Library.

4. Jose Alex Mathew, A.M.Khan, U.C. Niranjan, "Diagnosis of the Abnormality Extracted MRI slice Images of a GUI based Intelligent Diagnostic Imaging System", will be published in the conference proceeding by IEEE, which will be included in IEEE Xplore. IEEE Catalog Number: CFP1166N-PRT, ISBN: 978-1-61284-762-7.

Publications- National

1. Jose Alex Mathew, A.M.Khan, U.C. Niranjan, "Link between GUI and MRI Images in an Intelligent Diagnostic MRI Imaging System", Proceedings of National conference on Communication, Control and Computing, 2011, (NCCP-2011), ISBN: 978-93-80697-91-8.

Paper presented -International

1. Jose Alex Mathew, A.M.Khan, U.C. Niranjan, "Digital Image Processing Methods to find the Abnormalities of the Brain for the Development of Intelligent Diagnostic Imaging System", Proceedings of International Conference on VLSI and Communication, SAINTGITS College of Engineering, Kottayam, 2009, pp. 1009-1014.

2. Jose Alex Mathew, A.M.Khan, U.C. Niranjan, "Image Segmentation and Classification of the MRI Images to find the Abnormalities of the Brain for the Development of an Intelligent Diagnostic Imaging System", Proceedings of International conference on Electronic Design and Signal Processing 2009, ICEDSP 09 MIT Manipal.

3. Jose Alex Mathew, A.M.Khan, U.C. Niranjan, "Algorithms to find the thresholds for the Abnormality Extraction of the MRI slice Images of a GUI based Intelligent Diagnostic Imaging System", Proceedings of International Conference on VLSI, Communication and Instrumentation, SAINTGITS College of Engineering, Kottayam, April 7,8,9-2011.

4. Jose Alex Mathew, A.M.Khan, U.C. Niranjan, "Diagnosis of the Abnormality Extracted MRI slice Images of a GUI based Intelligent Diagnostic Imaging System", IEEE International Conference on Process Automation, Control and Computing (IPACC2011), 20-22 July 2011 at CIT, Coimbatore.

Paper presented -National

1. Jose Alex Mathew, A.M.Khan, U.C. Niranjan, "An Intelligent Imaging System for MRI Scan", Proceedings of National Conference on devices, Intelligent System and Communication, MITDIC-2007, MIT Manipal.

2. Jose Alex Mathew, A.M.Khan, U.C. Niranjan, "Clinical Study of the Abnormalities of Brain for the Development of Intelligent Diagnostic Imaging System", Proceedings of Fifth National Control Instrumentation System Conference, CISCON-2008, MIT Manipal.

3. Jose Alex Mathew, A.M.Khan, U.C. Niranjan, "Link between GUI and MRI Images in an Intelligent Diagnostic MRI Imaging System", Proceedings of National conference on Communication, Control and Computing, 2011, (NCCP-2011), St Joseph Engineering College, Mangalore.

References

[1] Dr. Joseph P Hernak. "The basics of MRI".

[2] Scott W. Atlas, " Magnetic Resonance Imaging of the Brain and Spine (2 Volume Set)".

[3] Gregory A. Hance, Scott E. Umbaugh, Randy H. Moss , and Iana William V. Stoecker, "Unsupervised Color Image Segmentation", *IEEE Engineering In Medicine And Biology*, pp. 104-111, January/February 1996.

[4] N. Manousakas, P. E. Undrill, G. G. Cameron, and T. W. Readpath, "Split-And-Merge Segmentation Of Magnetic Resonance Medical Images: Performance Evaluation And Extension To Three Dimensions", *Computers And Biomedical Research*, pp. 393-412, 1996.

[5] Koen Van Leemput, Frederik Maes, Dirk Vandermeulen, and Paul Suetens, "A Unifying Framework For Partial Volume Segmentation Of Brain MR Images", *IEEE Transactions On Medical Imaging*, Vol. 22, No. 1, pp. 105 - 119, January 2003.

[6] Nilanjan Ray, Scott T. Acton, Talissa Altes, Eduard E. De Lange, and James R. Brookeman "Merging Parametric Active Contours Within Homogeneous Image Regions For MRI-Based Lung Segmentation" *IEEE Transactions On Medical Imaging*, Vol.22, No. 2, pp.189-198, February 2003.

[7] Yoshinobu Sato, Hisashi Tanaka, Takashi Nishii, and Katsuyuki Nakanishi, "Limits On The Accuracy Of 3-D Thickness Measurement In Magnetic Resonance Images—Effects Of Voxel Anisotropy", *IEEE Transactions On Medical Imaging*, Vol. 22, No. 9, pp. 1076-1088, September 2003.

[8] Julio Carballido-Gamio, Serge J. Belongie, and Sharmila Majumdar, "Normalized Cuts In 3-D For Spinal MRI Segmentation", *IEEE Transactions On Medical Imaging*, Vol. 23, No. 1, pp. 36 –44, January 2004

[9] Yalin Zheng, Mark S. Nixon, and Robert Allen, "Automated Segmentation Of Lumbar Vertebre In Digital Videofluoroscopic Images", *IEEE Transactions On Medical Imaging*, Vol. 23, No. 1, pp. 45-52, , January 2004

[10] V. Grau, A. U. J. Mewes, M. Alcaniz, R. Kikinis, and S. K. Warfield "Improved Watershed Transform For Medical Image Segmentation Using Prior Information" *IEEE Transactions On Medical Imaging*, Vol. 23, No. 4, pp. 447-458, April 2004.

[11] Meritxell Bach Cuadra, Claudio Polio, Anton Bardera, Olivier Cuisenaire, Jean-Guy Villemure, and Jean-Philippe Thiran, "Atlas-Based Segmentation Of Pathological Mr Brain Images Using A Model Of Lesion Growth" *IEEE Transactions On Medical Imaging*, Vol. 23, No, 10, pp.1301-1314, October 2004.

[12] Albert C. S. Chung, J. Alison Noble, and Paul Summers "Vascular Segmentation Of Phase Contrast Magnetic Resonance Angiograms Based On Statistical Mixture Modeling And Local Phase Coherence" *IEEE Transactions On Medical Imaging*. Vol. 23, No. 12, pp.1490-1507, December 2004.

[13] Abdolah Chalechale, Golshah Naghdy, and Alfred Mertins, "Sketch-Based Image Matching Using Angular Partitioning", *IEEE Transactions On Systems, Man, And Cybernetics—Part A: Systems And Humans*, Vol. 35, No. 1, pp. 28-41, January 2005.

[14] Sokratis Makrogiannis, George Economou, Spiros Fotopoulos, and Nikolaos G. Bourbakis "Segmentation Of Color Images Using Multiscale Clustering And Graph Theoretic Region Synthesis", *IEEE Transactions On Systems, Man, And Cybernetics—Part A: Systems And Humans*, Vol. 35, No. 2, pp. 224-238, March 2005.

[15] M. Lynch, O. Ghita, and P.F. Whelan, "Automatic Segmentation Of The Left Ventricle Cavity And Myocardium In MRI Data", *Computers In Biology And Medicine* 36, pp. 389-407, 2006.

[16] Ying Zhuge, Jayaram K. Udupa, and Punam K. Saha "Vectorial Scale-Based Fuzzy-Connected Image Segmentation" *Computer Vision And Image Understanding*, 101, pp. 177-193, 2006.

[17] Ludovic Macaire, Nicolas Vandenbroucke, and Jack-Gerard Postaire, "Color Image Segmentation By Analysis Of Subset Connectedness And Color Homogeneity Properties", *Computer Vision And Image Understanding*, 102, pp. 105-116, 2006.

[18] Raz Koren, and Yitzhak Yitzhaky, "Automatic Selection Of Edge Detector Parameters Based On Spatial And Statistical Measures", *Computer Vision And Image Understanding*, 102, pp.204-213, 2006.

[19] Hemg-Hua Chang, Daniel J. Valentino, Gary R. Duckwiler, and Arthur W. Toga, "Segmentation Of Brain MR Images Using A Charged Fluid Model", *IEEE Transactions On Biomedical Engineering*, Vol. 54, No. 10, pp. 1798-1813, October 2007.

[20] Francois Chabaf, David M. Hansell, and Guang-Zhong Yang " Computerized Decision Support In Medical Imaging Challenges In Using Image Processing And Automated Feature Extraction For Improving Diagnostic Accuracy", *IEEE Engineering In Medicine And Biology*, pp.89-96, September/October 2000.

[21] Alex P. Zijdenbos, Reza Forghani, and Alan C. Evans "Automatic Pipeline Analysis Of 3-D MRI Data For Clinical Trials: Application To Multiple Sclerosis", *IEEE Transactions On Medical Imaging*, Vol. 21, No. 10, pp.1280-1291, October 2002.

[22] Chuin-Mu Wang, Clayton Chi-Chang Chen, Yi-Nung Chung, Sheng-Chih Yang, Pau-Choo Chung, Ching-Wen Yang and Chein-I. Chang, "Detection Of Spectral Signatures In Multispectral MR Images For Classification", *IEEE Transactions On Medical Imaging*, Vol. 22, No. 1, pp.50-61, January 2003.

[23] Gholam-Ali Hossein-Zadeh, Hamid Soltanian-Zadeh, and Babak A. Ardekani, "Multiresolution fMRI Activation Detection Using Translation Invariant Wavelet Transform And Statistical Analysis Based On Resampling", *IEEE Transactions On Medical Imaging*, Vol. 22, No. 3, pp.302-314, March 2003.

[24] Jeffrey Tsao "Interpolation Artifacts In Multimodality Image Registration Based On Maximization Of Mutual Information", *IEEE Transactions On Medical Imaging*, Vol. 22, No. 7, pp.854-864, , July 2003.

[25] Gholam-Ali Hossein-Zadeh, Babak A. Ardekani, and Hamid Soltanian-Zadeh, "Activation Detection In fMRI Using A Maximum Energy Ratio Statistic Obtained By Adaptive Spatial Filtering", *IEEE Transactions On Medical Imaging*, Vol. 22, No. 7, pp. 795-805, October 2007.

[26] P. Hellier, C. Barillol, I. Corouge, B. Gibaud, G. Le Goualher, D. L. Collins, A. Evans. G. Malandain, N. Ayache, G. E. Chrislensen, and H. J. Johnson, "Retrospective Evaluation Of Intersubject Brain Registration", *IEEE Transactions On Medical Imaging*, Vol. 22, No. 9, pp.1120-1130, September 2003.

[27] Xavier Descombes, Frithjof Kruggel, Gert Wollny, and Hermann Josef Gertz, "An Object-Based Approach For Detecting Small Brain Lesions: Application To Virchow-Robin Spaces", *IEEE Transactions On Medical Imaging*, Vol. 23, No. 2, pp.246-255, February 2004.

[28] Christopher L. Gilchrist, Jessie Q. Xia, Lori A. Setton, and Edward W. Hsu, "High-Resolution Determination Of Soft Tissue Deformations Using MRI And First-Order Texture Correlation", *IEEE Transactions On Medical Imaging*, Vol. 23, No. 5, pp. 546- 553, May 2004.

[29] Thomas Netsch, and Arianne Van Muiswinkel, "Quantitative Evaluation Of Image-Based, Distortion Correction In Diffusion Tensor Imaging", *IEEE Transactions On Medical Imaging*, Vol. 23, No. 7, pp. 789-798, July 2004.

[30] Chih-Ping Wei, Paul Jen-Hwa Hu, Olivia R. Liu Sheng, and Yen-Hsien Lee, "Intelligent Image Prefetching For Supporting Radiologist's Primary Reading: A Decision-Rule Inductive Learning Approach", *IEEE Transactions On Systems, Man, And Cybernetics—Part A: Systems And Humans*, Vol. 35, No. 2, pp. 261-274, March 2005.

[31] Judy R. James, Karmen K. Yoder, Olaniyi Osuntokun, Andrew Kalnin, Askiel Bruno, and Evan D. Moms, "A Supervised Method For Calculating Perfusion/Diffusion Mismatch Volume In Acute Ischemic Stroke", *Computers In Biology And Medicine*, 36, pp. 1268-1287, 2006.

[32] Marcelo Kleber Felisberto, Heitor Silverio Lopes, and Tania Mezzadri, "An Object Detection And Recognition System For Weld Bead Extraction From Digital Radiographs", Computer Vision And Image Understanding, 102, pp. 238-249, 2006.

[33] V.S.N. Prasad, Larry S. Davis, Son Dinh Tran, and Ahmed Elgammal, "Edge Affinity For Pose-Contour Matching", *Computer Vision And Image Understanding*, 104, pp.36-47, 2006.

[34] Celia Varela, Pablo G. Tahoces, Arturo J. Mendez, Miguel Souto, and Juan J. Vidal "Computerized Detection Of Breast Masses In Digitized Mammograms", *Computers In Biology And Medicine*, 37, pp.214-226, 2007.

[35] Samuel Kadoury, and Martin D. Levine, "Face Detection In Gray Scale Images Using Locally Linear Embeddings", *Computer Vision And Image Understanding*, 105, pp.1-20, 2007.

[36] Wael Badawy, Michael Weeks, Guoqing Zhang, Michael Talley, and Magdy A. Bayoumi, " MRI Data Copression Using A 3-D Discrete Wavelet Transform", *IEEE Engineering In Medicine And Biology*, pp.35-57, July/August 2002.

[37] Ersin Bayram, Yaorong Ge, and Christopher L Wyatt, "Confidence-Based Anisotropic Filtering Of Magnetic Resonance Images" , *IEEE Engineering In Medicine And Biology*, pp. 156-160, September/October 2002.

[38] Aleksandra Pizurica, Wilfried Philips, Ignace Lemahieu, and Marc Acheroy, "A Versatile Wavelet Domain Noise Filtration Technique For Medical Imaging", *IEEE Transactions On Medical Imaging*. Vol. 22, No. 3, pp.323-331, March 2003

[39] Temujin Gautama, Danilo P. Mandic, and Marc M. Van Hulle, "Signal Nonlinearity In fMRI: A Comparison Between BOLD And MION", *IEEE Transactions On Medical Imaging*, Vol. 22, No. 5, pp. 636-645, May 2003.

[40] Ralf Mekle, Andrew F. Laine, and Ed X. Wu, "Combined MR Data Acquisition Of Multicontrast Images Using Variable Acquisition Parameters And K-Space Data Sharing", *IEEE Transactions On Medical Imaging*, Vol. 22, No. 7, pp.806-823, July 2003.

[41] Paul Bao, and Ip Zhang, "Noise Reduction For Magnetic Resonance Images Via Adaptive Multiscale Products Thresholding", *IEEE Transactions On Medical Imaging*, Vol. 22, No. 9, pp.1089-1099, September 2003.

[42] Pierre Gravel, Gilles Beaudoin, and Jacques A. De Guise, "A Method For Modeling Noise In Medical Images", *IEEE Transactions On Medical Imaging*, Vol. 23, No. 10, pp. 1221-1232, October 2004.

[43] Bing Keong Li, Bin Xu, Feng Liu, and Stuart Crozier, "Multiple-Acquisition Parallel Imaging Combined With A Transceive Array For The Amelioration Of High-Field RF Distortion: A Modeling Study", *Wiley Periodicals, Magnetic Resonance Part B*, 29B, pp. 95-105, 2006.

[44] Victor Taracila, Labros S. Petropoulos, Timothy P. Eagan, and Robert W. Brown, "Image Uniformity Improvement For Birdcage-Like Volume Coils At 400 Mhz Using Multichannel Excitations", *Wiley Periodicals, Magnetic Resonance Part B*, 29B, pp. 153-160, 2006.

[45] Kai-Qi Huang, Qiao Wang, and Zhen-Yang Wu, "Natural Color Image Enhancement And Evaluation Algorithm Based On Human Visual System", *Computer Vision And Image Understanding, Elsevier*, 103, pp. 52-63, 2006.

[46] Berkman Sahiner, and Andrew E. Yagle, " Iterative Inversion Of The Radon Transform", *IEEE Engineering In Medicine And Biology*, pp. 112 -117, September/October 1996.

[47] Mukund Desai, Rami Mangoubi, Jayant Shah, William Karl, Homer Pien, Andrew Worth, and David Kennedy, "Functional MRI Activity Characterization Using Response Time Shift Estimates From Curve Evolution", *IEEE Transactions On Medical Imaging*, Vol.21, No.11, pp.1402-1412, Nov 2002.

[48] Dinggang Shen, and Christos Davatzikos, "HAMMER: Hierarchical Attribute Matching Mechanism For Elastic Registration", *IEEE Transactions On Medical Imaging*, Vol. 21, No. 11, pp.1421-1439, November 2002.

[49] Thorsten Schormann, and Matthias Kraemer, "Voxel-Guided Morphometry (VGM) And Application To Stroke", *IEEE Transactions On Medical Imaging*, Vol. 22, No. 1, pp. 62-74, January 2003.

[50] T. Hartkens, D. L. G. Hill, A. D. Castellano-Smith, D. J. Hawkes, C. R. Maurer, A. J. Martin, W. A. Hall, H. Liu, and C. L. Truwit, "Measurement And Analysis Of Brain Deformation During Neurosurgery", *IEEE Transactions On Medical Imaging*, Vol. 22. No. 1, pp. 82-92, 2003.

[51] Kirk W. Finnis, Yves P. Starreveld, Andrew G. Parrent, Abbas F. Sadikot, and Terry M. Peters, "Three-Dimensional Database Of Subcortical Electrophysiology For Image-Guided Stereotactic Functional Neurosurgery", *IEEE Transactons On Medical Imaging*, Vol. 22, No. 1, pp. 93-104, January 2003.

[52] Bradley P. Sutton, Douglas C. Noll, and Jeffrey A. Fessler, " Fast, Iterative Image Reconstruction For MRI In The Presence Of Field Inhomogeneities", *IEEE Transactions On Medical Imaging*, Vol. 22, No. 2, pp. 178-188, 2003.

[53] Laszlo G. Nyiil, Jayaram K. Udupa, and Puriam K. Saha, "Incorporating A Measure Of Local Scale In Voxel-Based 3-D Image Registration", *IEEE Transactions On Medical Imaging*, Vol. 22, No. 2, pp.228-237, February 2003.

[54] Julia A. Schnabel, Christine Tanner, Andy D. Castellano-Smith, Andreas Degenhard, Martin O. Leach, D. Rodney Hose, Derek L. G. Hill, and David J. Hawkes, " Validation Of Nonrigid Image Registration Using Finite-Element Methods: Application To Breast MR Images", *IEEE Transactions On Medical Imaging*, Vol. 22, No. 2, pp. 238-247, February 2003.

[55] Nasser Fatouraee, and Amir A. Amini, "Regularization Of Flow Streamlines In Multislice Phase-Contrast MR Imaging", *IEEE Transactions On Medical Tmaging*, Vol. 22, No. 6, pp. 699-709, June 2003.

[56] Torsten Rohlfing, Calvin R. Maurer, David A. Bluemke, and Michael A. Jacobs, "Volume-Preserving Nonrigid Registration Of MR Breast Images Using Free-Form Deformation With An Incompressibility Constraint", *IEEE Transactions On Medical Imaging*, Vol. 22, No. 6, pp. 730-741, June 2003.

[57] Francois G. Meyer, and Jatuporn Chinrungrueng, "Analysis Of Event-Related fMRI Data Using Best Clustering Bases", *IEEE Transactions On Medical Imaging*, Vol. 22, No. 8, pp.933-939, August 2003.

[58] Josien P. W. Pluim J. B. Antoine Maintz, and Max A. Viergever, " Mutual-Information-Based Registration Of Medical Images: A Survey", *IEEE Transactions On Medical Imaging*. Vol. 22, No. 8, pp.986-1004, August 2003.

[59] James S Duncan, and Lawrence H. Staib, "Image Processing And Analysis At IPAG", *IEEE Transactions On Medical Imaging*, Vol. 22, No. 12, pp. 1505-1518, December 2003.

[60] Sea Chen, Charles A. Bouman, and Mark J. Lowe, " Clustered Components Analysis For Functional MRI", *IEEE Transactions On Medical Imaging*, Vol. 23, No. 1, pp. 85-97, January 2004.

[61] C. Studholme, V. Cardenas, E. Song, F. Ezekiel. A. Maudsley, and M. Weiner, "Accurate Template-Based Correction Of Brain MRI Intensity Distortion With Application To Dementia And Aging", *IEEE Transactions On Medical Imaging*, Vol. 23, No. 1, pp.99-110, January 2004.

[62] Christian F. Beckmann, and Stephen M. Smith, " Probabilistic Independent Component Analysis For Functional Magnetic Resonance Imaging", *IEEE Transactions On Medical Imaging*, Vol. 23, No. 2, pp. 137-152, February 2004.

[63] Mark W. Woolrich, Mark Jenkinson, J. Michael Brady, and Stephen M. Smith, "Fully Bayesian Spatio-Temporal Modeling Of fMRI Data", *IEEE Transactions On Medical Imaging*, Vol. 23, No. 2, pp. 213-231, February 2004.

[64] Hamid Soltanian-Zadeh, Donald J. Peck, David O. Hearshen, and Renee R. Lajiness-O'neill, " Model-Independent Method For fMRI Analysis", *IEEE Transactions On Medical Imaging*, Vol. 23, No. 3, pp. 285-296, March 2004.

[65] Alle Meije Wink, and Jos B. T. M. Roerdink, "Denoising Functional MR Images: A Comparison Of Wavelet Denoising And Gaussian Smoothing", *IEEE Transactions On Medical Imaging*, Vol. 23, No. 3, pp.374-387, March 2004.

[66] Edward H. Herskovits, Hanchuan Peng, and Christos Davatzikos, "A Bayesian Morphometry Algorithm", *IEEE Transactions On Medical Imaging*, Vol. 23, No.6, pp.723-737, June 2004.

[67] J.-F. Mangin, D. Riviere, A. Cachia, E. Duchesnay, Y. Cointepas, D. Papadopoulos-Orfanos, D. L. Collins, A. C. Evans, and J. Regis, "Object-Based Morphometry Of The Cerebral Cortex", *IEEE Transactions On Medical Imaging*, Vol. 23, No. 8, pp. 968-982, August 2004.

[68] Chad W. Washington, and Michael I. Miga, "Modality Independent Elastography (MIE): A New Approach To Elasticity Imaging", *IEEE Transactions On Medical Imaging*, Vol. 23, No. 9, pp. 1117-1128, September 2004.

[69] Zhong Xue, Dinggang Shen, and Christos Davatzikos, "Determining Correspondence In 3-D MR Brain Images Using Attribute Vectors As Morphological", *IEEE Transactions On Medical Imaging*, Vol. 23, No. 10, pp. 1276 -1291, October 2004.

[70] Kris Luyten, Jan Van Den Bergh, Chris Vandervelpen, and Karin Coninx, "Designing Distributed User Interfaces For Ambient Intelligent Environments Using Models And Simulations", *Computers & Graphics, Elsevier*, 30, pp. 702- 713, 2006.

[71] Anant Madabhushi, Jayaram K. Udupa, and Andre Souza, "Generalized Scale: Theory, Algorithms, And Application To Image Inhomogeneity Correction", *Computer Vision And Image Understanding, Elsevier*, 101, pp.100-121, 2006.

[72] Marek'r. Ogiela, Ryszard Tadeusiewicz, and Lidia Ogiela, "Graph Image Language Techniques Supporting Radiological, Hand Image Interpretations", *Computer Vision And Image Understanding, Elsevier*, 103, pp. 112-120, 2006.

[73] James W. Woods, Charles A. Sneiderman, Kamran Hameed, Michael J. Ackerrnan, and Charlie Hatton, "Using UMLs Metathesaurus Concepts To Describe Medical Images: Dermatology Vocabulary", *Computers In Biology And Medicine*, 36, pp.89-100,2006.

[74] Huaien Luo , and Sadasivan Puthusserypady, "fMRI Data Analysis With Nonstationary Noise Models: A Bayesian Approach", *IEEE Transactions On Biomedical Engineering*, Vol. 54, No. 9, pp. 1621-1630, September 2007.

[75] Pascal Haigron, Gerard Le Berre, and Jean Louis Coatrieux, "3D Navigation In Medicine- Virtual Sensor Modelling And Image Rendering", *IEEE Engineering In Medicine And Biology*, pp. 70-78, March/April1996.

[76] Gilbert R. Hillman, Chih-Wei Chang, Hao Ying, John Yen, Leena Ketonen, and Thomas A. Kent, "A Fuzzy Logic Approach To Identifying Brain Structures In MRI Using Expert Anatomic Knowledge", *Computers And Biomedical Research*, 32, pp. 503-516, 1999.

[77] E. Mark Haacke, and Zhi-Pei Liang, "Challenges Of Imaging Structure And Function With MRI", *IEEE Engineering In Medicine And Biology*, pp. 55-68, 2000.

[78] Ernest V. Garcia, Tracy L Faber, James R. Gait, C. David Cooke, and Russell D. Folks, "Advances In Nuclear Emission Pet And Spect Imaging", *IEEE Engineering In Medicine And Biology*, pp. 21 - 33, September/October 2000.

[79] Stephen J. Riederer , "Current Technical Development Of MRI", *IEEE Engineering In Medicine And Biology*, pp.34-41, Sep/Oct 2000.

[80] Robert Turner, and Roger J. Ordidge, "Technical Challenges Of Functional Magnetic Resonance Imaging", *IEEE Engineering In Medicine And Biology*, pp. 42- 54, September/October 2000.

[81] Theobald O.J. Fuchs, Marc Kachelriefi, and Willi A. Kalender, "System Performance Of Multislice Spiral Computed Tomography, A Technique That Provides Significantly Improved Image Quality With Drastically Reduced Scan Times", *IEEE Engineering In Medicine And Biology*, pp. 63-70, September/October 2000.

[82] David M. Hansell, "Imaging The Lungs With CT", *IEEE Engineering In Medicine And Biology*, pp. 71 – 79, September/October 2000.

[83] Peng Wen, and Yan Li, "Constructing Head Models By Computation", *IEEE Engineering In Medicine And Biology*, pp. 82-87, November/December 2000.

[84] Pernilla Selskog, Einar Heiberg, Tino Ebbers, Lars Wigstrom, and Matts Karlsson , " Kinematics Of The Heart: Strain-Rate Imaging From Time-Resolved Three-Dimensional Phase Contrast MRI", *IEEE Transactions On Medical Imaging*, Vol. 21, No. 9, pp.1105-1109, September 2002.

[85] Jiann-Der Lee, Chung-Hsien Huang, and Shih-Tseng Lee, "Improving Stereotactic Surgery Using 3-D Reconstruction, Combining Image Processing, Computed Tomography Data, And A 3-D Brain Atlas For Automating And Improving The Efficiency Of Neurosurgery", *IEEE Engineering In Medicine And Biology*, pp.109-116, November/December 2002.

[86] Hanhua Feng, Hong Gu, David Silbersweig, Emily Stern, and Yihong Yang, "Single-Shot MR Imaging Using Trapezoidal-Gradient-Based Lissajous Trajectories", *IEEE Transactions On Medical Imaging*, Vol. 22, No. 8, pp. 925-932, August 2003.

[87] C. A. Piron, P. Causer, R. Jong, R. Shumak, and D. B. Plewes, "A Hybrid Breast Biopsy System Combining Ultrasound And MRI", *IEEE Transactionson Medical Imaging*, Vol. 22, No. 9, pp.1100-1110, September 2003.

[88] Nicholas Ayache, "Epidaure: A Research Projects Medical Image Analysis, Simulation, and Robotics at INRIA", *IEEE Transactions On Medical Imaging*, Vol. 22, No. 10, PP1185-1201, October 2003.

[89] Shigeyuki Suzuki, Naoki Suzuki, Asaki Hattori, Akihiko Uchiyama, and Susumu Kobayashi, "Sphere-Filled Organ Model For Virtual Surgery System", *IEEE Transactions On Medical Imaging*, Vol. 23, No. 6, pp.714-722, June 2004.

[90] Mohan Manubhai Trivedi, , Kohsia Samuel Huang, and Ivana Mikic, "Dynamic Context Capture And Distributed Video Arrays For Intelligent Spaces", *IEEE Transactions On Systems, Man, And Cybernetics—Part A: Systems And Humans*, Vol. 35, No. 1, pp. 145-163, January 2005.

[91] Dimitra D. Dionysiou, Georgios S. Stamatakos, Nikolaos K. Uzunoglu, and Konstantina S. Nikita, "A Computer Simulation Of In Vivo Tumour Growth And Response To Radiotherapy: New Algorithms And Parametric Results", *Computers In Biology And Medicine*, 36, pp. 448-464, 2006.

[92] Jose M Perez-Sanchez, Ignacio Rodriguez, Rigoberto Perez De Ale, Manuel Cortijo, and Jesus Ruiz-Cabello, "C0MSPIRA3D: A Combined Approach To Radial And Spiral 3D MRI", *Wiley Periodicals*, 29B, pp. 20-27, 2006.

[93] Daniel Gareis, Thomas Neuberger, Volker C. Behr, Peter M. Jakob, Cornelius Faber, and Mark A. Gr1swold, "Transmit-Receive Coil-Arrays At 17.6t, Configurations for ^{1}H, ^{23}NA, And ^{31}P MRI", *Wiley Periodicals, Concepts Magnetic Resonance Part B*, 29B, pp. 20-27, 2006.

[94] M. Sabati, M.L. Lauzon, N. Nagarajappa, and R. Frayne, "A Real-Time 3D Large Field-Of-View MRI System With Interactive Table Motion", *Wiley Periodicals Inc. Concepts Magnetic Resonance Part B , 29B*, pp. 28-41, 2006

[95] Michael R. Lamprecht, David M. Sabatini, and Anne E. Carpenter, "Cellprofiler: Free, Versatile Software For Automated Biological Image Analysis" *Biotechniques, 42*, pp. 71-75, January 2007.

[96] Khaled Z. Abd-Elmoniem, Smita Sampath, Nael F. Osman, and Jerry L. Prince, "Real-Time Monitoring Of Cardiac Regional Function Using Fastharp MRI And Region-Of-Interest Reconstruction" , *IEEE Transactions On Biomedical Engineering*, Vol. 54, No. 9, pp. 1650-1656, September 2007.

[97] Stergios Paiamas, Dimitris Kalivas, and Ourania Panou-Diamandi, "An Internet-Based System For The Commerce Of Medical Devices, A Portal For Improving Communication Between Healthcare Professionals And The Medical Device Industry", *IEEE Engineering In Medicine And Biology*, pp. 26 -33, March/April 2002.

[98] Mark Rossman, Malek Adjouadi, Melvin Ayala, and Ilker Yaylali, "An Interactive Interface For Seizure Focus Localization Using Spect Image Analysis", *Computers In Biology And Medicine*, 36, pp. 70-88, 2006.

[99] Silvio Antonio Carro, and Jacob Scharcanski, "A Framework For Medical Visual Information Exchange On The Web", *Computers In Biology And Medicine*, 36, pp. 327-338, 2006.

[100] Otsu. N, "A Threshold Selection Method from Gray-Level Histograms," *IEEE Transactions on. Systems, Man, and Cybernetics*, vol. SMC-9, no. 1, pp. 62-66, 1979.

[101]Russ, J. C.. The Image Processing Handbook, 3rd ed., *CRC Press*, Boca Raton, FL.

[102] Rafael C. Gonzalez, Richard E. Woods: "Digital Image Processing 2: 567-638.

[103]Anne G Osborn, Published by Amirsys(tm) , "Diagnostic Imaging: Brain".

[104]Peter H. Abrahams, Jonathan D. Spratt, Lonie R Salkowski, "Imaging Atlas of Human Anatomy".

[105]Jeff Ross, Michael Brant-Zawadzki, Mark Chen, Kevin Moore, Karen Salzman, "Diagnostic Imaging: Head &Neck".

[106]Anne G. Osborn , "Diagnostic Neuroradiology" .

[107]Ric Harnsberger, Patricia Hudgins, Richard Wiggins, Christian Davidson , "Diagnostic Imaging: Head and Neck".

[108]Canny. J. , "A Computational Approach for Edge Detection," *IEEE Transactions on Pattern Anal. Machine Intell*, vol. 8, No. 6, pp. 679-698, 1986.

[109] Soille, P, " Morphological Image Analysis: Principles and Applications". 2nd ed.. *Springer-Verlag, NY*, 2003.

[110]Vincent, L., "Morphological Grayscale Reconstruction in Image Analysis: Applications and Efficient Algorithms," *IEEE Transactions on Image Processing* vol. 2, no. 2, pp. 176-201. 1993.

[111]Natick, MA "Using MATLAB, Version 6.5,The MathWorks, Inc".

[112] Rafael C. Gonzalez, Richard E. Woods, Steven L. Eddins: "Digital Image Processing Using MATLAB : 378-425.

[113]Vincent, L. and Soille, P., "Watersheds in Digital Spaces: An Efficient Algorithm Based on Immersion Simulations, " *IEEE Transactions on Pattern Anal Machine Intell*, vol. 13, no. 6, pp. 583-598, 1991.

[114]Marchand Patrick, Holland Thomas O., "Graphics and GUIs with Matlab", 3ed, *CRC Press*, 2003.

[115] www.ewh.ieee.org

[116] www.mathwork.com

[117] www.ob.ultrasound.net

[118]www.radiologyinfo.org